Gauge freedom, quantum measurements, and time-dependent interactions in cavity QED

Alessio Settineri,[1] Omar Di Stefano,[1,2] David Zueco,[3] Stephen Hughes,[4] Salvatore Savasta,[1,*] and Franco Nori[2,5]

[1]*Dipartimento di Scienze Matematiche e Informatiche, Scienze Fisiche e Scienze della Terra, Università di Messina, I-98166 Messina, Italy*

[2]*Theoretical Quantum Physics Laboratory, RIKEN Cluster for Pioneering Research, Wako-shi, Saitama 351-0198, Japan*

[3]*Instituto de Ciencia de Materiales y Nanociencia de Aragón and Departamento de Física de la Materia Condensada, CSIC-Universidad de Zaragoza, Pedro Cerbuna 12, 50009 Zaragoza, Spain*

[4]*Department of Physics, Engineering Physics, and Astronomy, Queen's University, Kingston, Ontario, Canada K7L 3N6*

[5]*Physics Department, The University of Michigan, Ann Arbor, Michigan 48109-1040, USA*

(Received 27 December 2019; revised 23 December 2020; accepted 5 April 2021; published 28 April 2021)

The interaction between quantized electromagnetic fields in cavities and natural or artificial atoms has played a crucial role in developing our understanding of light-matter interactions and quantum technologies. Recently, new regimes beyond the weak and strong light-matter coupling of cavity-QED have been explored in several settings, wherein the light-matter coupling rate becomes comparable to (ultrastrong coupling) or even exceeds (deep-strong coupling) the photon frequency. These ultrastrong coupling regimes can give rise to new physical effects and applications, and they challenge our understanding of cavity QED; fundamental issues like the proper definition of subsystems, their quantum measurements, the structure of light-matter ground states, and the analysis of time-dependent interactions are subject to gauge ambiguities that lead to even qualitatively distinct predictions. The resolution of these ambiguities is important for understanding and designing next-generation quantum devices that can operate in extreme coupling regimes. Here we discuss and provide solutions to these ambiguities by adopting an approach based on operational procedures involving measurements on the individual light and matter components of the interacting system.

DOI: 10.1103/PhysRevResearch.3.023079

I. INTRODUCTION

Ultrastrong coupling (USC) between light and matter [1,2] can be achieved by coupling many dipoles (collectively) to light, or by using matter systems like superconducting artificial atoms whose coupling is not bound by the small size of the fine-structure constant. The largest light-matter coupling strengths have been measured in experiments with Landau polaritons in semiconductor systems [3] and in setups with superconducting quantum circuits [4]. Another potentially promising route to realize USC with natural atoms and molecules is by using metal resonators, since the coupling rates are not bound by diffraction. Single molecules in plasmonic cavities are starting to enter the USC regime [5], and two-dimensional transition metal dichalcogenides (TMDs) coupled to metal particles have already reached the USC regime [6], even at room temperature. Ultrastrong plasmon exciton interactions has also been reported with crystallized films of carbon nanotubes [7]. The physics of the USC regime can also be accessed by using quantum simulation approaches [8].

These very strong interaction regimes are also a test bed for gauge invariance [9–12]. The issue of gauge invariance, pointed out as early as 1952 by Lamb [13], has consistently affected the theoretical predictions in atomic physics and in nonrelativistic quantum electrodynamics (QED) (see, e.g., Refs. [14–17]). Recently, it has been shown that the standard quantum Rabi model, describing the coupling between a TLS and a single-mode quantized electromagnetic field, heavily violates this principle in the presence of ultrastrong light-matter coupling [9,10]. This issue has been recently solved by introducing a generalized minimal-coupling replacement [11,12,18].

Here we investigate the consequences of the restored gauge invariance of the quantum Rabi model on measurable predictions. Specifically, (i) we provide example calculations of gauge-invariant photodetection rates; (ii) we show how the qubit dispersive readout is modified by its ultrastrong interaction with an electromagnetic resonator; and (iii) we eliminate gauge ambiguities in the description of virtual excitations and light-matter entanglement in the ground state of the quantum Rabi Hamiltonian.

Concerning point (i), we analyze the gauge invariance of Glauber's formula [19] for the photodetection probability. We focus on the calculation of the emission rate for a quantum Rabi system prepared in two different low-energy excited states. According to Glauber's photodetection theory, the detection rate for photons polarized along a direction i is proportional to $\langle\psi|\hat{E}_i^{(-)}\hat{E}_i^{(+)}|\psi\rangle$, where $\hat{\mathbf{E}}^{(\pm)}$ are the positive and negative frequency components of the electric-field

*Corresponding author: ssavasta@unime.it

operator. In the Coulomb gauge, $\hat{\mathbf{E}}$ is proportional to the field canonical momentum and can be expanded in terms of photon operators. In contrast, in the multipolar gauge, the canonical momentum that can be expanded in terms of photon operators is not $\hat{\mathbf{E}}$ but the displacement field operator $\hat{\mathbf{D}}$ [17]. Consequently, in the multipolar gauge the electric field operator associated to a cavity mode cannot be expanded in terms of photon operators only. In the context of the Dicke model, describing the interaction of several (two-level) atoms with a single cavity mode, it has been shown that ignoring this issue can lead to incorrect results [20,21]. This subtlety, originating from the gauge dependence of the field canonical momentum (see, e.g., Refs. [14,15,17]), is generally disregarded in the quantum Rabi model [1], and the usual procedure is to obtain the system states in the dipole gauge (the multipolar gauge after the electric-dipole approximation) $|\psi_D\rangle$, and to calculate the photodetection rate ignoring that in this gauge the electric field operator is not a canonical momentum. As we show here, this procedure, when applied to the quantum Rabi model, can lead to strongly incorrect (and unphysical) predictions.

The qubit dispersive readout, (ii), represents an important example of quantum-nondemolition measurement. Coupling a quibit with moderate interaction strength to an out-of-resonance electromagnetic resonator, it is possible to obtain information on the qubit state without affecting it too much. In this case, the situation with respect to point (i) is reversed, since, in the multipolar gauge the particle momentum is not affected by the interaction, in contrast to to the Coulomb gauge.

Finally, with point (iii), we face gauge ambiguities related to the presence of ground state excitations. A distinguishing feature of USC systems is the presence of entangled light and matter excitations in the ground state, determined by the counter-rotating terms in the interaction Hamiltonian [22–24]. Indeed, all excited states are also dressed by multiple virtual excitations [25]. Much research on these systems has dealt with understanding whether these dressed excitations are real or virtual and how they can be probed or extracted [1,2]. These vacuum excitations can be converted into real detectable ones (see, e.g., Refs. [25–31]). However, the analysis of these effects is affected by possible ambiguities arising from the gauge dependence of the system eigenstates [10,11,32]. Specifically, the unitary gauge transformation does not conserve virtual excitations, nor light-matter entanglement [32]. Hence, the definition of these key features of the USC regime is subject to "ambiguities," so that, as we show here, a maximally entangled ground state can become separable in a different gauge. In particular, we show that the entangled light and matter excitations in the ground state, that can be observed (e.g., after a sudden switch-off of the interaction), are those calculated in the Coulomb gauge. Hence the existence of a correct quantum Rabi model in the Coulomb gauge is essential to calculate these quantities.

The analysis of points (i)–(iii) in this paper shows that the gauge-invariant quantum Rabi model is an essential tool to provide correct testable predictions not affected by gauge ambiguities. Although we present numerical results for TLSs interacting with a single mode electromagnetic resonator, the concepts and methods developed here are far more general. For example, they can also be applied to general multilevel matter systems and multimode resonators.

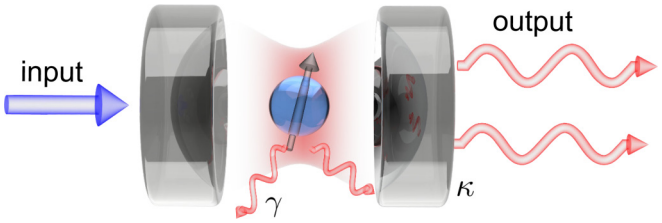

FIG. 1. Cavity QED setup. Schematic view of a typical cavity QED system consisting of an atom (depicted as an effective spin) embedded in an optical cavity. The symbols γ and κ represent the atom and cavity decay rates, respectively.

II. QUANTUM RABI HAMILTONIANS

In this section, we briefly recall the quantum Rabi model, focusing on the Hamiltonians in the Coulomb gauge and dipole gauge, and on the transformations relating the two different gauges.

Let us consider a simple cavity QED system represented by a single atom (dipole) coupled to an optical resonator (see Fig. 1). We start by adopting the Coulomb gauge, where the particle momentum is coupled only to the transverse part of the vector potential $\hat{\mathbf{A}}$. It represents the field coordinate, while its conjugate momentum is proportional to the transverse electric field operator. The latter field (as well as the vector potential) can be expanded in terms of photon creation and destruction operators: $\hat{\mathbf{E}}_C(\mathbf{r},t) = \sum_k \mathbf{E}_k(\mathbf{r})\hat{a}_k e^{-i\omega_k t} + \text{H.c.}$, where $\mathbf{E}_k(\mathbf{r}) = \sqrt{\hbar\omega_k/2\varepsilon_0}\,\mathbf{f}_k(\mathbf{r})$ are the effective mode amplitudes, and H.c. represents Hermitian conjugate. Here, $\mathbf{f}_k(\mathbf{r})$ are any general "normal modes" with real eigenfrequencies, ω_k, obtained from Maxwell's equations for a particular medium. They are normalized and complete (including also the longitudinal modes, $\omega_k = 0$), so that $\sum_k \epsilon_b(\mathbf{r}')\mathbf{f}_k^*(\mathbf{r})\mathbf{f}_k(\mathbf{r}') = \mathbf{1}\delta(\mathbf{r}-\mathbf{r}')$, where ϵ_b is the relative dielectric function of a background dielectric medium. The system Hamiltonian is

$$\hat{H}_C = \frac{1}{2m}[\hat{\mathbf{p}}_C - q\hat{\mathbf{A}}(\mathbf{r})]^2 + V(\mathbf{r}) + \sum_k \hbar\omega_k \hat{a}_k^\dagger \hat{a}_k, \qquad (1)$$

where $\hat{\mathbf{p}}_C$ and $V(\mathbf{r})$ are the particle's canonical momentum and potential.

The quantum Rabi Hamiltonian in the Coulomb gauge, can be obtained considering a single two-level system (TLS) at position $\mathbf{r}_0$, with (real) dipole moment $\boldsymbol{\mu} = q\langle e|\mathbf{x}|g\rangle$, interacting with a single cavity mode $[(\hat{a}_k, \mathbf{f}_k, \omega_k) \to (\hat{a}, \mathbf{f}_c, \omega_c)]$. The correct (namely, satisfying the gauge principle) quantum Rabi Hamiltonian [11] strongly differs from the standard quantum Rabi model, and takes the modified form

$$\hat{\mathcal{H}}_C = \hbar\omega_c \hat{a}^\dagger\hat{a} + \frac{\hbar\omega_0}{2}\{\hat{\sigma}_z \cos[2\eta(\hat{a}+\hat{a}^\dagger)] + \hat{\sigma}_y \sin[2\eta(\hat{a}+\hat{a}^\dagger)]\}, \qquad (2)$$

where $\omega_c\eta \equiv g = \sqrt{\omega_c/2\hbar\epsilon_0}\,\boldsymbol{\mu}\cdot\mathbf{f}_c(\mathbf{r}_0)$, and $\hat{\sigma}_j$ are the usual Pauli operators. Very recently, this result has been obtained by using a different approach based on the implementation of the gauge principle in TLSs [18]; this alternative procedure can be regarded as the two-site version of the general method used to implement the gauge principle in lattice gauge theories [33,34]. In quantum field theory, the coupling of particles with

the electromagnetic field is introduced to guarantee that the theory is invariant under a local (in space and time) phase transformation of the particle's wave function. The changes in the particle's equation of motion (or in the action) are compensated by introducing a coupling with the field, by the so-called minimal coupling replacement. When the particle's wave function undergoes such a local phase change, the field transforms according to a gauge transformation, so that the action of the total system remains unchanged. It has been shown that approximations such as the truncation of the Hilbert space for the matter system can cause a violation of the gauge principle, thus breaking gauge invariance. Such a breaking is particularly dramatic when the matter system is truncated to only two quantum states (quantum Rabi model), and the light-matter coupling is very strong (USC). The method developed in Ref. [11], leading to Eq. (2) provides one resolution to this issue.

In cavity QED, the multipolar gauge followed by the dipole approximation (dipole gauge) represents a convenient and widely used choice. A generic system operator in the multipolar gauge, $\hat{O}_M$, is related to the corresponding operator in the Coulomb gauge $\hat{O}_C$ by a suitable unitary Power-Zienau-Woolley (PZW) transformation [17,35]: $\hat{O}_M = \hat{T}\hat{O}_C\hat{T}^\dagger$ (see Appendix A). It turns out that in the multipolar gauge, while the field coordinate remains unchanged, its conjugate momentum is $\hat{\mathbf{\Pi}}_M = -\epsilon_0\epsilon_b(\mathbf{r})\hat{\mathbf{E}}_M - \hat{\mathbf{P}} = -\hat{\mathbf{D}}_M$, where $\hat{\mathbf{P}}$ is the electric polarization and $\hat{\mathbf{D}}_M$ is the displacement field [14,36,37], which can be directly expanded in terms of photon operators, using

$$\hat{\mathbf{F}}_M(\mathbf{r},t) \equiv \frac{\hat{\mathbf{D}}_M(\mathbf{r},t)}{\epsilon_0\epsilon_b(\mathbf{r})} = i\sum_k \sqrt{\frac{\hbar\omega_k}{2\epsilon_0}}\mathbf{f}_k(\mathbf{r})\hat{a}_k(t) + \text{H.c.}, \quad (3)$$

where $\hat{\mathbf{F}}_M$ is the effective electric field that atomic dipoles couple to [37]. For a single dipole at position $\mathbf{r}_0$, the interaction Hamiltonian is $H_I = -q\boldsymbol{x}\cdot\hat{\mathbf{F}}(\mathbf{r}_0) + (qx)^2/\epsilon_0\epsilon_b(\mathbf{r}_0)$. Considering a single TLS, we obtain

$$\hat{\mathbf{F}}_D(\mathbf{r}) = \hat{\mathbf{E}}_D(\mathbf{r}) + \frac{\boldsymbol{\mu}}{\epsilon_0\epsilon_b(\mathbf{r}_0)}\delta(\mathbf{r}-\mathbf{r}_0)\,\hat{\sigma}_x, \quad (4)$$

where $\hat{\mathbf{E}}_D(\mathbf{r})$ is the electric field operator in the dipole gauge. We note that for spatial locations away from the dipole ($\mathbf{r} \neq \mathbf{r}_0$), then $\hat{\mathbf{F}}_D$ and $\hat{\mathbf{E}}_D$ are equivalent. Next, we rewrite $\hat{\mathbf{E}}_D(\mathbf{r})$ in a way that makes each mode contribution clear:

$$\hat{\mathbf{E}}_D(\mathbf{r},t) = i\sum_k \sqrt{\frac{\hbar\omega_k}{2\epsilon_0}}\mathbf{f}_k(\mathbf{r})\hat{a}_k(t) + \text{H.c.} - \frac{1}{2\epsilon_0}\left[\sum_k \mathbf{f}_k^*(\mathbf{r})\mathbf{f}_k(\mathbf{r}_0) + \mathbf{f}_k^*(\mathbf{r}_0)\mathbf{f}_k(\mathbf{r})\right]\cdot\boldsymbol{\mu}\,\hat{\sigma}_x. \quad (5)$$

We now consider the single-mode limit, which is typically assumed in models such as the quantum Rabi model, where a single-mode cavity is the dominant mode of interest (see Appendix A):

$$\hat{\mathbf{E}}_D(\mathbf{r},t) = i\sqrt{\frac{\hbar\omega_c}{2\epsilon_0}}\mathbf{f}_c(\mathbf{r})\hat{a}'(t) + \text{H.c.}, \quad (6)$$

where $\hat{a}'(t) = \hat{a}(t) + i\eta\hat{\sigma}_x(t)$ (see Ref. [11]). We observe that the operators $\hat{a}'$ and $\hat{a}'^\dagger$ obey the same commutation relations of the bosonic operators $\hat{a}$ and $\hat{a}^\dagger$. The total Hamiltonian (throughout the paper we use the calligraphic font for operators projected in a two level space) in the dipole gauge is

$$\hat{\mathcal{H}}_D = \hat{\mathcal{H}}_{\text{free}} + \hat{\mathcal{V}}_D, \quad (7)$$

where $\hat{\mathcal{H}}_{\text{free}} = \hbar\omega_c\hat{a}^\dagger\hat{a} + \frac{\hbar\omega_0}{2}\hat{\sigma}_z$, ω_0 is the transition frequency of the TLS, and the interaction Hamiltonian is

$$\hat{\mathcal{V}}_D = i\eta\hbar\omega_c(\hat{a}^\dagger - \hat{a})\hat{\sigma}_x. \quad (8)$$

The two gauges are related by the transformation $\hat{\mathcal{H}}_D = \hat{\mathcal{T}}\hat{\mathcal{H}}_C\hat{\mathcal{T}}^\dagger$, where $\hat{\mathcal{T}} = \exp(i\hat{\mathcal{F}})$ with $\hat{\mathcal{F}} = -\eta\hat{\sigma}_x(\hat{a}+\hat{a}^\dagger)$ (see Appendix A).

III. PHOTODETECTION

Gauge ambiguities may affect the calculation of photodetection probabilities. As anticipated in Sec. I, this issue originates from the gauge dependence of the field's canonical momentum (see, e.g., Refs. [14,15,17]). Reference [11] pointed out the gauge dependence of the photon creation and annihilation operators, without quantifying the impact of such dependence on photodetection rates. In this section, we face this problem by considering two different approaches. We first start from analyzing the gauge invariance of Glauber's formula for the photodetection probability. Then, we analyze a specific model of photodetectors: frequency-tunable two-level sensors; they constitute a powerful computational tool for calculating normal-order field correlation functions. Moreover, we clarify the origin of the gauge issues and how to fix then, by exploring gauge transformations of the whole quantum system consisting of an USC system plus one or more sensors (which can act as point detectors).

A. Gauge invariance of photodetection probabilities

The photon rate that can be measured from a pointlike detector in the resonator, at the position $\mathbf{r}$ and at a given time t, is proportional to [19]

$$\langle\hat{\mathbf{E}}^{(-)}(\mathbf{r},t)\cdot\hat{\mathbf{E}}^{(+)}(\mathbf{r},t)\rangle, \quad (9)$$

where $\hat{\mathbf{E}}^{(+)}$ and $\hat{\mathbf{E}}^{(-)}$ are the positive and negative frequency components of the electric-field operator, with $\hat{\mathbf{E}}^{(-)} = [\hat{\mathbf{E}}^{(+)}]^\dagger$. In the Coulomb gauge, the electric-field operator $\hat{\mathbf{E}}$ is proportional to the field canonical momentum and can be expanded in terms of photon operators. However, in the multipolar gauge, the canonical momentum that can be expanded in terms of photon operators is not $\hat{\mathbf{E}}$ but the displacement operator $\hat{\mathbf{D}}$ (as mentioned earlier). Also note that, in the absence of interactions, or when the rotating-wave approximation can be applied to the interaction Hamiltonian, the positive-frequency operator only contains photon destruction operators. However, when the rotating-wave approximation cannot be applied, this direct correspondence does not hold [38]. By using standard input-output theory, analogous results for the rate of emitted photons can be obtained for a detector placed outside the cavity [28,39].

Considering a single-mode resonator coupled to a TLS (quantum Rabi model), assuming that the system is prepared

initially in a specific energy eigenstate $|j_C\rangle$, and using Eq. (9), then the resulting detection rate in the Coulomb gauge is proportional to

$$W = \sum_{k<j} |\langle k_C|\hat{\mathcal{P}}|j_C\rangle|^2, \tag{10}$$

where

$$\hat{\mathcal{P}} = i(\hat{a} - \hat{a}^\dagger), \tag{11}$$

and we ordered the eigenstates so that $j > k$ for eigenfrequencies $\omega_j > \omega_k$. If a tunable narrow-band detector is employed, a single transition can be selected, so that the detection rate for a frequency $\omega = \omega_{j,k} \equiv \omega_j - \omega_k$ is proportional to

$$W_{j,k} = |\langle k_C|\hat{\mathcal{P}}|j_C\rangle|^2. \tag{12}$$

In contrast, in the dipole gauge, we obtain

$$W_{j,k} = |\langle k_D|i(\hat{a} - \hat{a}^\dagger) - 2\eta\hat{\sigma}_x|j_D\rangle|^2. \tag{13}$$

The gauge principle, as well as the theory of unitary transformations, ensures that Eqs. (12) and (13) provide the same result [11]. In constrast, the usual procedure, consisting in using the dipole gauge without changing accordingly the field operator (see, e.g., Refs. [1,2]): $W'_{j,k} = |\langle k_D|i(\hat{a} - \hat{a}^\dagger)|j_D\rangle|^2$, provides wrong results. When the normalized coupling strength $\eta \ll 1$, the error can be small. However, when η is non-negligible, W and W' can provide very different predictions, as shown explicitly in Fig. 2. Figure 2(a) displays the energy differences between the lowest excited levels and the ground energy level of the quantum Rabi Hamiltonian $\hat{\mathcal{H}}_C$ (or $\hat{\mathcal{H}}_D$) for the case of zero cavity-atom detuning ($\omega_c = \omega_0$). Here we indicate the dressed ground state as $|\tilde{0}\rangle$, and the excited states as $|\tilde{n}\pm\rangle$ on the basis of the usual notation for the Jaynes-Cummings (JC) eigenstates $|n\pm\rangle$ (see, e.g., Ref. [40]). Figure 2(b) shows that, except for negligible couplings (where $W_{\tilde{1}\pm,\tilde{0}} = W'_{\tilde{1}\pm,\tilde{0}} = 0.5$), $W_{\tilde{1}\pm,\tilde{0}}$ and $W'_{\tilde{1}\pm,\tilde{0}}$ display different results. The differences are evident already for $\eta \sim 0.1$.

It is interesting to point out some noteworthy features of this comparison. First, we observe that $W_{\tilde{1}+,\tilde{0}} > W_{\tilde{1}-,\tilde{0}}$ for all the values of η, and finally, for increasing η, $W_{\tilde{1}-,\tilde{0}} \to 0$. These results originate from the dependence on η of the corresponding transition frequencies $\omega_{\tilde{1}\pm,\tilde{0}}$. Specifically, photodetection is an energy absorbing process, whose rate is proportional to the intensity, which in turn is proportional to the energy of the absorbed photons. Hence, $\omega_{\tilde{1}+,\tilde{0}} > \omega_{\tilde{1}-,\tilde{0}}$ implies $W_{\tilde{1}+,\tilde{0}} > W_{\tilde{1}-,\tilde{0}}$. For the same reason, when $\omega_{\tilde{1}-,\tilde{0}} \to 0$, there is no energy to be absorbed, and $W_{\tilde{1}-,\tilde{0}} \to 0$. On the contrary, $W'_{\tilde{1}\pm,\tilde{0}}$ displays the opposite (*unphysical*) behavior.

Finally, we remark that, very recently, it has been shown [41] that the detection rate $W_{j,k}$ in Eq. (12) provides very different results with respect to $X_{j,k} = |\langle k_C|\hat{\mathcal{Q}}|k_C\rangle|^2$, which is the corresponding quantity obtained using a different quadrature: $\hat{\mathcal{Q}} = \hat{a} + \hat{a}^\dagger$. The form of this interaction also affects the observables calculated in a quantum master equation approach, such as the cavity emitted spectrum of a pump-driven quantum Rabi model [42].

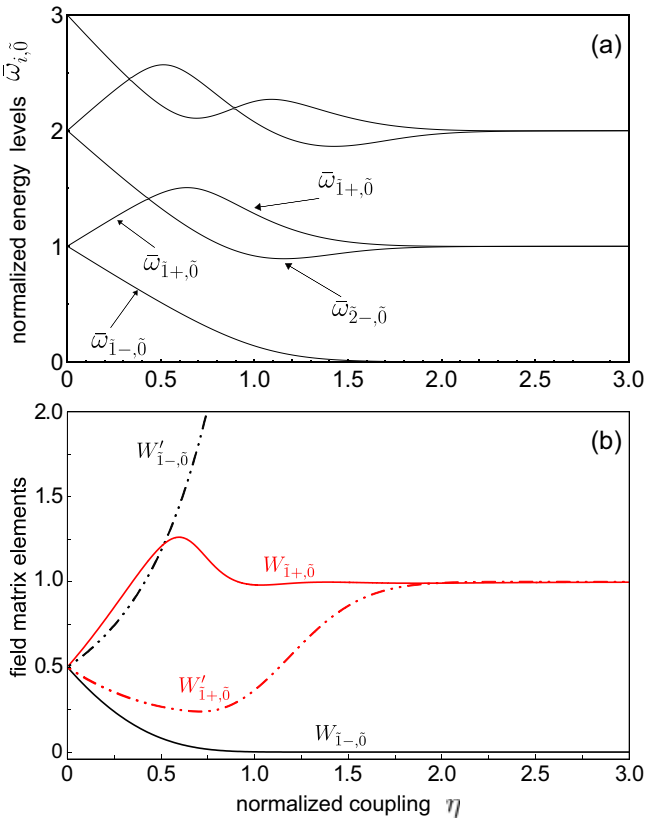

FIG. 2. Quantum Rabi model. (a) Normalized energy levels differences between the lowest excited levels and the ground energy level of the quantum Rabi Hamiltonian $\hat{\mathcal{H}}_C$ for the case of zero detuning ($\omega_c = \omega_0$) as a function of the normalized coupling strength η; (b) modulus squared of the transition matrix elements of the electric-field operator, $W_{\tilde{1}\pm,\tilde{0}}$, accounting for the transitions between the two lowest excited levels and the ground state of the quantum Rabi Hamiltonian, vs η. For comparison, the panel also reports the wrong matrix elements $W'_{\tilde{1}\pm,\tilde{0}}$ (see text).

B. Two-level sensors

It has been shown [43] that normal-order correlation functions, which describe the detection of photons according to Glauber's theory, can be calculated considering frequency-tunable two-level sensors in the limit of their vanishing coupling with the field. The rate at which the sensor's population grows corresponds to the photodetection rate. If two or more sensors are included, their joint excitation rates provides information on normal-order multiphoton correlations.

This procedure can also be applied when the electromagnetic field interacts strongly with a matter system so that the counter-rotating terms in the interaction Hamiltonians cannot be neglected. Let us consider a simple USC system that consists of an electromagnetic single-mode resonator strongly interacting with a TLS with normalized coupling strength η. Then we also consider a two-level sensor interacting with the resonator with vanishing coupling $\eta_s \ll \eta$. The standard cavity-sensor interaction Hamiltonian in the dipole gauge is written as [43]

$$\hat{V}'_{\rm dg} = -i\hbar\omega_c\eta_s(\hat{a} - \hat{a}^\dagger)\hat{\sigma}^s_x. \tag{14}$$

If the USC system is prepared in a state $|j\rangle$ and the sensor has a resonance frequency $\omega_s = \omega_{jl}$ $(l < j)$, by applying the Fermi golden rule, then the excitation rate of the sensor is proportional to

$$|\langle l_D|\hat{\mathcal{P}}|j_D\rangle|^2, \tag{15}$$

where $|j_D\rangle$ is a system eigenstate in the dipole gauge and $\hat{\mathcal{P}} = i(\hat{a} - \hat{a}^\dagger)$. This result, however, is different from what can be obtained within the Coulomb gauge: $W_{lj} = |\langle l_C|\hat{\mathcal{P}}|j_C\rangle|^2$.

It is instructive to find the origin of such gauge ambiguity and to solve it. Actually, in the dipole gauge, the interaction energy between the field and the sensor is $-\int d^3r\, \hat{\mathbf{E}} \cdot \hat{\mathbf{P}}_s$, where $\hat{\mathbf{P}}_s = \boldsymbol{\mu}\hat{\sigma}_x^s$ is the sensor polarization. Using the relation $\hat{\mathbf{E}} = (\hat{\mathbf{D}} - \hat{\mathbf{P}})/\epsilon_0$ (we here assume $\epsilon_b(\mathbf{r}) = 1$), the total Hamiltonian in the dipole gauge can be written as

$$\hat{\mathcal{H}}_{\rm dg} = \hat{\mathcal{H}}_{\rm dg}^{\rm USC} + \hat{\mathcal{H}}_s + \hat{\mathcal{V}}_{\rm dg}^s, \tag{16}$$

where $\hat{\mathcal{H}}_{\rm dg}^{\rm USC}$ is the system Hamiltonian in the absence of the sensor, $\hat{\mathcal{H}}_s = (\hbar\omega_s/2)\hat{\sigma}_z^s$, and

$$\hat{\mathcal{V}}_{\rm dg}^s = -\frac{1}{\epsilon_0}\int d^3r \hat{\mathbf{D}} \cdot \boldsymbol{\mu}\, \hat{\sigma}_x^s + \frac{1}{\epsilon_0}\int d^3r \hat{P}^2, \tag{17}$$

where

$$\hat{\mathbf{P}} = \boldsymbol{\mu}\hat{\sigma}_x + \boldsymbol{\mu}_s\hat{\sigma}_x^s, \tag{18}$$

is the total polarization. By expanding $\hat{\mathbf{D}}$ in terms of the photon operators, and using the relationship

$$\frac{1}{2}\sum_k [\mathbf{f}_k^*(\mathbf{r})\mathbf{f}_k(\mathbf{r}') + \mathbf{f}_k^*(\mathbf{r}')\mathbf{f}_k(\mathbf{r})] = \mathbf{1}\delta(\mathbf{r}-\mathbf{r}'), \tag{19}$$

and after neglecting the terms proportional to the qubits identities, we obtain

$$\hat{\mathcal{V}}_{\rm dg}^s = \sum_k \hbar\omega_k\eta_k^s[i(\hat{a}_k^\dagger - \hat{a}_k) + 2\eta_k\hat{\sigma}_x]\hat{\sigma}_x^s. \tag{20}$$

In the single-mode limit, this simplifies to

$$\hat{\mathcal{V}}_{\rm dg}^s = \hbar\omega_c\eta^s[i(\hat{a}^\dagger - \hat{a}) + 2\eta\hat{\sigma}_x]\hat{\sigma}_x^s. \tag{21}$$

Equation (21) differs from Eq. (14) only for the field-induced qubit-sensor interaction term, arising from the self-polarization terms in the dipole-gauge light-matter interaction Hamiltonian [44]. However, *it is precisely this term that ensures gauge invariance*: applying the Fermi golden rule, by using Eq. (21), instead of Eq. (14), we obtain the gauge invariant result

$$|\langle l_D|\hat{\mathcal{P}} - 2\eta\hat{\sigma}_x|j_D\rangle|^2 = |\langle l_C|\hat{\mathcal{P}}|j_C\rangle|^2 \equiv W_{lj}. \tag{22}$$

IV. READOUT OF A STRONGLY COUPLED QUBIT

While in the Coulomb gauge, the atom momentum is affected by the coupling with the field [17] [$m\dot{\mathbf{x}} = \hat{\mathbf{p}}_C - q\hat{\mathbf{A}}(\mathbf{x})$], in the dipole gauge it is interaction-independent: $m\dot{\mathbf{x}} = \hat{\mathbf{p}}_D$. This feature can give rise to ambiguities in the definition of the physical properties of an atom interacting with a field [16]. Moreover, an unambiguous separation between light and matter systems becomes problematic with increasing coupling strength. Again, we address this problem by adopting an operational approach based on what is actually measured. In cavity and circuit QED, quantum-non-demolition measurements are widely used [45–50]. Specifically, a quantum-non-demolition-like readout of the qubit can be realized by coupling it, with a moderate coupling strength, to a resonator mode b with a detuned resonance frequency $\omega_b \neq \omega_0$ (dispersive regime). The readout can be accomplished by detecting the dispersive qubit state-dependent shift of the resonator frequency: $\omega_b \to \omega_b + \chi\langle\hat{\sigma}_z\rangle$, where $\chi = \omega_b^2\eta_b^2/(\omega_0 - \omega)$ (see Fig. 3) [48,51–53]. If the qubit is coupled very strongly to a second field mode a, this readout scheme can provide interesting information on how the qubit state is affected by the USC regime. However, the expectation value $\langle\hat{\sigma}_z\rangle$ for a qubit in the USC regime is ambiguous when the coupling becomes sufficiently strong. Specifically, since $\langle\psi_C|\hat{\sigma}_z|\psi_C\rangle \neq \langle\psi_D|\hat{\sigma}_z|\psi_D\rangle$, the question arises which one of these two quantities is actually detected.

We start from the Hamiltonian in the Coulomb gauge (1), limited to include only two quantized normal modes (a and b). We then project the atomic system in order to consider two levels only, and assume for the resulting coupling strengths that $\eta_b \ll \eta_a$. The resulting Hamiltonian in the Coulomb gauge can be written as [11]

$$\hat{\mathcal{H}}_C = \hbar\omega_a\hat{a}^\dagger\hat{a} + \hbar\omega_b\hat{b}^\dagger\hat{b} + \frac{\hbar\omega_0}{2}\{\hat{\sigma}_z\cos[2\eta_a(\hat{a}^\dagger + \hat{a}) + 2\eta_b(\hat{b}^\dagger + \hat{b})] + \hat{\sigma}_y\sin[2\eta_a(\hat{a}^\dagger + \hat{a}) + 2\eta_b(\hat{b}^\dagger + \hat{b})]\}, \tag{23}$$

with $\eta_a = g_a/\omega_0$ and $\eta_b = g_b/\omega_0$. By using the angle transformation formulas, Eq. (23) becomes

$$\hat{\mathcal{H}}_C = \hbar\omega_a\hat{a}^\dagger\hat{a} + \hbar\omega_b\hat{b}^\dagger\hat{b} + \frac{\hbar\omega_0}{2}\hat{\sigma}_z\{\cos[2\eta_a(\hat{a}^\dagger + \hat{a})]\cos[2\eta_b(\hat{b}^\dagger + \hat{b})] - \sin[2\eta_a(\hat{a}^\dagger + \hat{a})]\sin[2\eta_b(\hat{b}^\dagger + \hat{b})]\} + \frac{\hbar\omega_0}{2}\hat{\sigma}_y\{\sin[2\eta_a(\hat{a}^\dagger + \hat{a})]\cos[2\eta_b(\hat{b}^\dagger + \hat{b})] + \cos[2\eta_a(\hat{a}^\dagger + \hat{a})]\sin[2\eta_b(\hat{b}^\dagger + \hat{b})]\}. \tag{24}$$

Furthermore, since $2\eta_b(\hat{b}^\dagger + \hat{b})$ is small, we can also apply the small-angle approximation $\cos(x) \simeq 1$, $\sin(x) \simeq x$, thus obtaining

$$\hat{\mathcal{H}}_C \simeq \hbar\omega_a\hat{a}^\dagger\hat{a} + \hbar\omega_b\hat{b}^\dagger\hat{b} + \frac{\hbar\omega_0}{2}\{\hat{\sigma}_z\cos[2\eta_a(\hat{a}^\dagger + \hat{a})] + \hat{\sigma}_y\sin[2\eta_a(\hat{a}^\dagger + \hat{a})]\} + \hbar\omega_0\eta_b(\hat{b}^\dagger + \hat{b})\{\hat{\sigma}_y\cos[2\eta_a(\hat{a}^\dagger + \hat{a})] - \hat{\sigma}_z\sin[2\eta_a(\hat{a}^\dagger + \hat{a})]\}. \tag{25}$$

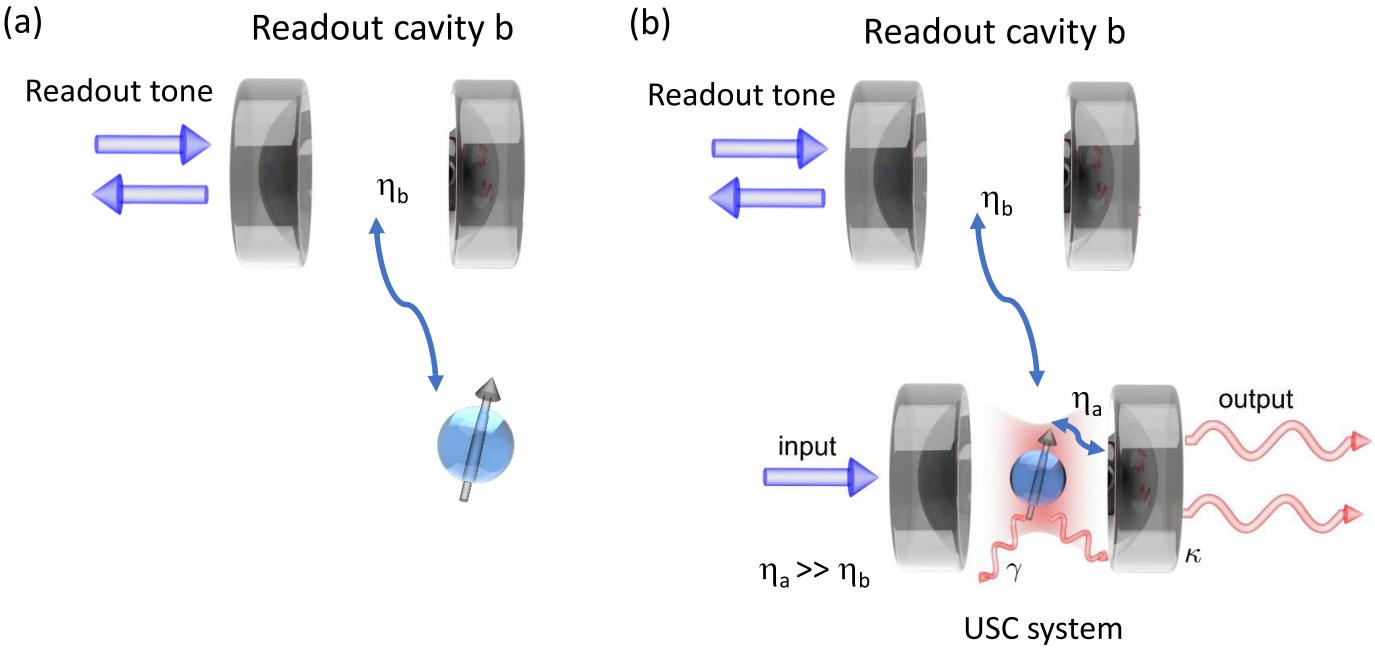

FIG. 3. Schematic view of dispersive readout of a two-level atom. The resonance frequency of the readout resonator is conditioned by the qubit state. Thus, by probing the resonance frequency of the resonator, e.g., by looking at the reflectivity of a readout tone, the qubit state can be determined. (a) Standard readout scheme of a bare two-level atom. (b) the same scheme for a two-level atom interacting with an additional resonator in the USC regime.

Introducing the Pauli operators in the Coulomb gauge:

$$\hat{\sigma}_x^C = \hat{\mathcal{T}}_a^\dagger \hat{\sigma}_x \hat{\mathcal{T}}_a = \hat{\sigma}_x, \tag{26a}$$

$$\hat{\sigma}_y^C = \hat{\mathcal{T}}_a^\dagger \hat{\sigma}_y \hat{\mathcal{T}}_a = \hat{\sigma}_y \cos[2\eta_a(\hat{a}^\dagger + \hat{a})] - \hat{\sigma}_z \sin[2\eta_a(\hat{a}^\dagger + \hat{a})], \tag{26b}$$

$$\hat{\sigma}_z^C = \hat{\mathcal{T}}_a^\dagger \hat{\sigma}_z \hat{\mathcal{T}}_a = \hat{\sigma}_z \cos[2\eta_a(\hat{a}^\dagger + \hat{a})] + \hat{\sigma}_y \sin[2\eta_a(\hat{a}^\dagger + \hat{a})], \tag{26c}$$

with $\hat{\mathcal{T}}_a = \exp[-i\eta_a \hat{\sigma}_x(\hat{a} + \hat{a}^\dagger)]$, Eq. (25) can be written in a more compact form as

$$\hat{\mathcal{H}}_C = \hbar\omega_a \hat{a}^\dagger \hat{a} + \hbar\omega_b \hat{b}^\dagger \hat{b} + \frac{\hbar\omega_0}{2}\hat{\sigma}_z^C + \eta_b \hbar\omega_0 (\hat{b}^\dagger + \hat{b})\hat{\sigma}_y^C. \tag{27}$$

It is important to note that, despite the $\hat{\sigma}_i^C$ operators also containing photon operators, their commutation rules remain unchanged: $[\hat{\sigma}_i^C, \hat{\sigma}_j^C] = 2i\epsilon_{ijk}\hat{\sigma}_k^C$.

At the beginning of this section we observed that while in the dipole gauge the particle's momentum is not affected by the light-matter interaction (in this gauge the interaction modifies the field momentum), in the Coulomb gauge the particle's momentum is affected (contrary to the field momentum). When reducing the full atom model to a two-dimensional Hilbert space, all this reflects into the gauge properties of the Pauli operators: while in the dipole gauge the operators $\hat{\sigma}_i$ are not modified by the interaction, in the Coulomb gauge $\hat{\sigma}_y^C$ and $\hat{\sigma}_z^C$ results are affected as shown in Eqs. (26b) and (26c).

If the USC system is in the state $|\psi_C\rangle$, starting from the Hamiltonian in Eq. (27), and applying the standard procedure for obtaining dispersive shifts [53], we find that the resonance frequency of the readout mode b is affected by the shift:

$$\chi \langle \psi_C | \hat{\mathcal{T}}_a^\dagger \hat{\sigma}_z \hat{\mathcal{T}}_a | \psi_C \rangle = \chi \langle \psi_D | \hat{\sigma}_z | \psi_D \rangle.$$

Hence, we can conclude that *the readout shift provides a measurement of the expectation value of the bare qubit population difference, as defined in the dipole gauge*. Interestingly, this measurement is able to provide direct information on the ground state qubit excitations induced by the interaction with resonator a.

The dot-dashed curves in Fig. 4 display the qubit excitation probabilities that can be measured by dispersive readout:

$$\langle i_C | \hat{\mathcal{T}}_a^\dagger \hat{\sigma}_+ \hat{\sigma}_- \hat{\mathcal{T}}_a | i_C \rangle = \langle i_D | \hat{\sigma}_+ \hat{\sigma}_- | i_D \rangle$$

for the ground state $|\tilde{0}\rangle$ of the quantum Rabi model and for the excited state $|\tilde{1}-\rangle$ (notice that $2\hat{\sigma}_+\hat{\sigma}_- = \hat{\sigma}_z + \hat{\mathcal{I}}$ where $\hat{\mathcal{I}}$, is the identity operator in the TLS space). We have also plotted (solid curves) $\langle i_C | \hat{\sigma}_+ \hat{\sigma}_- | i_C \rangle$ for the same states. As shown in Fig. 4, $\langle i_D | \hat{\sigma}_+ \hat{\sigma}_- | i_D \rangle$ strongly differs from $\langle i_C | \hat{\sigma}_+ \hat{\sigma}_- | i_C \rangle$. The latter, although not corresponding to what can measured in a readout measurement, has a precise physical meaning which will be described in the next section. An analytical description of these results in the large-coupling limit is provided in Appendix C.

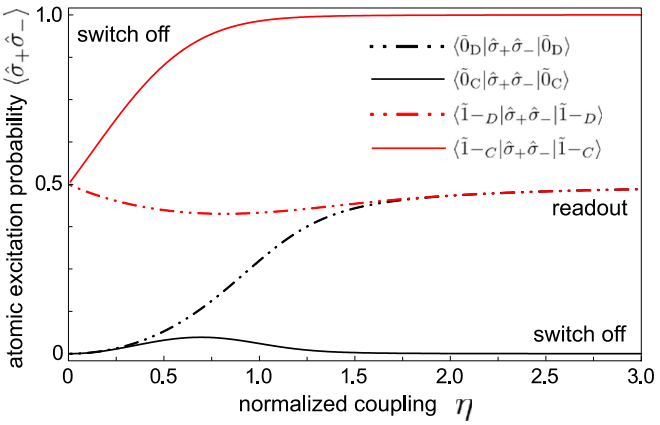

FIG. 4. Readout of a strongly coupled qubit. Qubit excitation probabilities for the system in its ground state (black curves) and in the first excited state (red curves), calculated in both the Coulomb (solid curves) and the dipole (dotted-dashed) gauges as a function of the normalized coupling strength η. Note that $\langle\hat{\sigma}_+\hat{\sigma}_-\rangle_D$ corresponds to what is measured via dispersive readout of the qubit (see Sec. IV). On the contrary, the photon rate released by the qubit after a sudden switch off of the light-matter interaction is proportional to $\langle\hat{\sigma}_+\hat{\sigma}_-\rangle_C$ (see Sec. V).

V. LIGHT-MATTER ENTANGLEMENT AND NONADIABATIC TUNABLE COUPLING

One of the most interesting features of USC systems is the presence of entangled ground states with virtual excitations [1,2]. However, since all the energy eigenstates of a cavity QED system are gauge dependent (e.g., $|\psi_D\rangle = \hat{\mathcal{T}}|\psi_C\rangle$), the mean number of excitations in the ground state are also gauge dependent. Moreover, the unitary operator $\hat{\mathcal{T}}$, enforcing gauge transformations, does not preserve the atom-field entanglement. Since physical observable quantities cannot be gauge dependent, the question arises if these ground state properties have any physical meaning.

It is known that these excitations, e.g., photons in the ground state, are unable to leave the cavity and can be regarded as virtual (see, e.g., Refs. [25,54]). Nevertheless, if the interaction is suddenly switched off (with switching time T going to zero), the system quantum state remains unchanged for regular Hamiltonians [55], and the excitations in the ground state can then evolve according to the free Hamiltonian and can thus be released and detected (see, e.g., Ref. [28]). Of course, *detectable* subsystem excitations and correlations have to be gauge invariant, since the results of experiments cannot depend on the gauge. On this basis, it should be possible to define gauge invariant excitations and qubit-field entanglement. A preliminary solution to this problem has been provided in Ref. [11]. In this section, we discuss this issue in more depth, providing a detailed analysis, and a solution to this problem.

It is instructive to analyze these quantities by adopting both the Coulomb gauge and the dipole gauge. We start with the Coulomb gauge. We consider the system initially prepared in its ground state $|\psi_C(t_0)\rangle = |\tilde{0}_C\rangle$. At $t = t_0$, the interaction is abruptly switched off within a time $T \to 0$. This nonadiabatic switch does not alter the quantum state [55], which at $t \geqslant t_1 = (t_0 + T)$ evolves as $|\psi_C(t)\rangle = \exp[-i\hat{\mathcal{H}}_{\rm free}(t - t_0)]|\psi_C(t_0)\rangle$. We can use this state to calculate, e.g., the observable mean photon number: $\langle\psi_C(t)|\hat{a}^\dagger\hat{a}|\psi_C(t)\rangle$, which can be measured by detecting the output photon flux from the resonator. It is worth noting that this expectation value can also be calculated by using the dipole gauge, by applying the unitary transformation to both the operator and the quantum states:

$$\langle\psi_C(t)|\hat{a}^\dagger\hat{a}|\psi_C(t)\rangle = \langle\psi_D(t)|\hat{a}'^\dagger\hat{a}'|\psi_D(t)\rangle.$$

The Hamiltonian in the dipole gauge can be obtained from that in the Coulomb gauge via a unitary transformation which, in this case becomes time-dependent. It can also be obtained by considering the corresponding gauge transformation of the field potentials, taking into account that, during the switch, the transformation depends explicitly on time. Carrying out the calculations in the dipole gauge (see also Appendix E), it can be shown that, even in the presence of a nonadiabatic switch off of the interaction, there are no gauge ambiguities if the explicit time dependence of the transformation (or of the generating function for the gauge transformation) is properly taken into account.

In order to test explicitly gauge invariance in the presence of ultrastrong interactions and nonadiabatic tunable couplings, we calculate the quantum state after a sudden switch off of the interaction, by using the dipole gauge. During the switch, the transformation is time-dependent and can be expressed as $\hat{\mathcal{T}}(t) = \exp[i\lambda(t)\hat{\mathcal{F}}]$, where $\lambda(t)$ is the switching function [with $\lambda(t) = 1$ for $t \leqslant t_0$, and $\lambda(t) = 0$ for $t \geqslant t_1$]. The resulting correct Hamiltonian in the dipole gauge is

$$\hat{\mathcal{H}}'_D(t) = \hat{\mathcal{H}}_{\rm free} + \hat{\mathcal{V}}_D(t) - \dot{\lambda}\hat{\mathcal{F}}. \tag{28}$$

For very fast switches, the last term in $\hat{\mathcal{H}}'_D(t)$ dominates during the switching and goes to infinity for switching times $T \to 0$. Hence its contribution to the time evolution during the switching time cannot be neglected. For switching times of the order of the coupling rate, the resulting Hamiltonian in the dipole gauge $\hat{\mathcal{H}}'_D(t)$ in Eq. (28) can differ significantly from the standard dipole-gauge Hamiltonian with time-independent parameters $\hat{\mathcal{H}}_D$ [see Eq. (7)].

Let us consider the system at $t = t_0$ (before the switch off) to be in the state $|\psi_D(t_0)\rangle$. Assuming $T \to 0$, just after the switch off ($t_1 = t_0 + T$), the resulting state is

$$|\psi_D(t_1)\rangle = \exp\left(i\hat{\mathcal{F}}\int_{t_0}^{t_1} dt\,\dot{\lambda}\right)|\psi_D(t_0)\rangle. \tag{29}$$

Since the integral is equal to -1, and $|\psi_D\rangle = \hat{\mathcal{T}}|\psi_C\rangle$, we obtain

$$|\psi_D(t_1)\rangle = \hat{\mathcal{T}}^\dagger|\psi_D(t_0)\rangle = |\psi_C(t_0)\rangle. \tag{30}$$

This result shows that, even in the presence of a nonadiabatic switch off of the interaction, there are no gauge ambiguities, since the final state (after the interaction has been switched off) does coincide with the corresponding state in the Coulomb gauge. The case where the system is prepared in the absence of interaction, which is then switched on and finally switched off before measurements, is analyzed in Appendix E.

In Ref. [32], it has been shown that the standard practice of adding a time dependence to the coupling rate gives rise, for sufficiently strong and nonadiabatic time-dependent

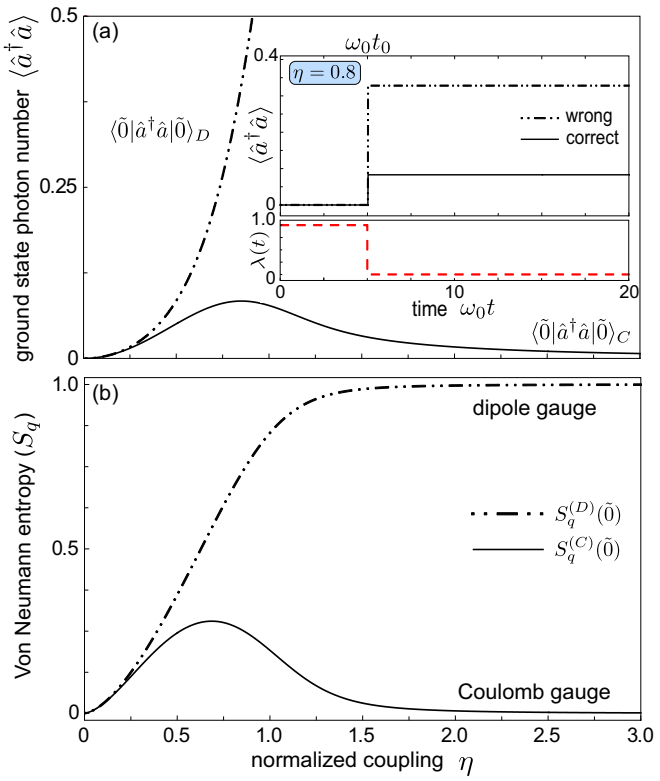

FIG. 5. Vacuum emission. (a) Mean photon number calculated in the Coulomb (solid curve) and in the wrong dipole (dot-dashed curve) gauges as a function of η for the system prepared in the ground state of the quantum Rabi model. (inset) Vacuum emission (mean photon number) after the switch off evaluated for $\eta = 0.8$. (b) Qubit entropies (which quantifies the qubit-oscillator entanglement) for the ground states (black curves) calculated in both the Coulomb (solid curves) and the wrong dipole (dotted-dashed) gauges as a function of the normalized coupling strength η.

interactions, to gauge-dependent predictions on final subsystem properties, such as the qubit-field entanglement or the number of emitted photons. This problem persists also when the system is prepared in the absence of any interaction, and measurements are carried out after switching off the coupling. Our analysis of gauge transformations in the presence of time-dependent interactions eliminates these ambiguities (see Appendix D).

Figure 5(a) displays the mean photon numbers $\langle \tilde{0}_C|\hat{a}^\dagger \hat{a}|\tilde{0}_C\rangle$ and $\langle \tilde{0}_D|\hat{a}^\dagger \hat{a}|\tilde{0}_D\rangle$. The first quantity is the correct one, calculated using the time evolution induced by $\hat{\mathcal{H}}_C(t)$. The latter is the wrong one, obtained considering the wrong dipole-gauge Hamiltonian $\hat{\mathcal{H}}_D(t) = \hat{\mathcal{T}}(t)\hat{\mathcal{H}}_C(t)\hat{\mathcal{T}}^\dagger(t)$ (see Appendix E). As shown in Fig. 5(b), the two mean values provide very different predictions for the observable mean photon number after the switch off. Very different predictions are also obtained for the qubit excitation probabilities (see Fig. 4).

Figure 5(b) displays the Von Neumann entropy S_q, which quantifies the qubit-oscillator entanglement for the system ground state (black curves) of the quantum Rabi model. The entropy [22] is obtained by calculating the ground state of the combined system $|\tilde{0}\rangle$, using it to obtain the qubit's reduced density matrix in the ground state $\rho_q = \mathrm{Tr}_{\mathrm{osc}}\{|\tilde{0}\rangle\langle\tilde{0}|\}$, and then evaluating the entropy of that state $S_q = -\mathrm{Tr}_{\mathrm{osc}}\{\rho_q \log_2 \rho_q\}$. The solid curves have been obtained using the Coulomb gauge, while the dotted-dashed ones, within the wrong dipole gauge [using $\hat{\mathcal{H}}_D(t)$]. It is interesting to observe that, for $\eta \gtrsim 0.2$, the degree of entanglement strongly differs in the two cases. In particular, while in the wrong dipole gauge both states become entangled cat states [56] displaying maximum entanglement above $\eta = 2$, S_q goes to zero in the Coulomb gauge, after reaching a maximum at $\eta \simeq 0.6$. These significant differences for large values of η can be understood by using an analytical approximation which works well for $\eta \gg 1$ (see Appendix C).

Although we applied this analysis to a TLS coupled to a single-mode resonator, the physical conclusions reached here are general (see Appendix D). Let us summarize the results discussed here considering a more general light-matter system. The correct Hamiltonian in the dipole gauge, in the presence of time-dependent interactions, is

$$\hat{H}'_D = \hat{T}(t)\hat{H}_C(t)\hat{T}^\dagger(t) + i\dot{\hat{T}}\hat{T}^\dagger, \tag{31}$$

where $\hat{H}_C$ is the Coulomb-gauge light-matter Hamiltonian in the absence of any Hilbert space truncation, while $\hat{T}$ is the time-dependent unitary operator enforcing the gauge transformation. In the absence of time-dependent interactions, $\hat{H}_C$ and the standard dipole-gauge Hamiltonian

$$\hat{H}_D \equiv \hat{T}\hat{H}_C\hat{T}^\dagger = \hat{H}'_D, \tag{32}$$

provide equivalent dynamics (notice that in the absence of time-dependent interactions, $\dot{\hat{T}} = 0$). In the presence of time-dependent interactions, only $\hat{H}'_D$ provides dynamical solutions which are equivalent to the ones determined by $\hat{H}_C$, and the standard multipolar Hamiltonian $\hat{H}_D$ loose its physical meaning and has to be disregarded. Consequently, *we can consider $\hat{H}_C$ more fundamental than $\hat{H}_D$*. The first ($\hat{H}_C$) originates directly from the minimal coupling replacement enforcing the gauge principle, while the latter ($\hat{H}_D$) results from the first, after a transformation which can be time-dependent.

A different point of view could be to consider, independently on the historical derivation, $\hat{H}_D$ as the fundamental Hamiltonian and deriving $\hat{H}_C$ from it after a time-dependent unitary transformation. In this case, the resulting Hamiltonian in the Coulomb gauge, providing a dynamics equivalent to that of $\hat{H}_D(t)$, would be

$$\hat{H}'_C(t) = \hat{T}^\dagger(t)\hat{H}_D(t)\hat{T}(t) + i\dot{\hat{T}}(t)^\dagger\hat{T}(t).$$

This Hamiltonian, owing to the second term on the right-hand side of the above equation, does not correspond to a minimal coupling replacement as prescribed by the gauge principle (see, e.g., Refs. [18,57]). Nevertheless, $\hat{H}_C$ is directly obtained by the minimal coupling replacement (which implements the gauge principle) after setting to zero the longitudinal component of the vector potential (which has no dynamical relevance) [17].

In summary, the main result of this section consists of an operational *definition of ground state excitations and entanglement in cavity-QED systems which is independent of gauge transformation*. The physical quantities that can be observed in experiments have to be calculated using the Coulomb gauge

Hamiltonian, or any other equivalent Hamiltonian obtained performing a time-dependent unitary transformation.

VI. DISCUSSION AND CONCLUSIONS

By adopting an approach based on operational procedures involving measurements, we have highlighted and solved a number of qualitative ambiguities in the theoretical description of cavity QED systems, especially important in USC regimes. Broadly, these results deepen our understanding of subtle, although highly relevant, fundamental aspects of the interaction between quantized fields and matter, and are also relevant for the design and development of new applications exploiting the unprecedented possibilities offered by the USC and DSC regimes (see, e.g., Refs. [1,58,59]).

Specifically, we have shown (Sec. III) that, if the transformation of the photon operators $\hat{a}$ and $\hat{a}^\dagger$ when using the dipole gauge is not taken into account, incorrect results are obtained, even at moderate coupling strengths. In Sec. IV, we have shown how to obtain the correct gauge-invariant qubit population which is measured under dispersive readout, when the qubit is coupled in the USC or DSC regimes with an additional electromagnetic resonator.

The states (e.g., the energy eigenstates) of a cavity-QED system are gauge dependent. As a consequence, the number of virtual excitations, as well as the degree of light-matter entanglement in the ground state, are gauge dependent. In Sec. V, we provided an operational definition of ground state excitations and entanglement in cavity-QED systems which is independent on gauge transformations. The physical quantities that can be experimentally observed after, e.g., the switch off of the interaction, have to be calculated using the Coulomb gauge Hamiltonian, or any other equivalent Hamiltonian obtained performing a time-dependent unitary transformation of the Coulomb-gauge Hamiltonian.

This work was motivated by the development of a gauge-invariant quantum Rabi model [11] and by the possibility to implement the gauge principle in truncated Hilbert spaces [11,18]. Our paper has focused on the quantum Rabi model describing individual two-level systems, whose interaction with light is introduced via the minimal coupling replacement. So far, the USC regime has been reached only in systems involving several emitters or in superconducting circuits galvanically coupled to microwave resonators. As a consequence, the specific numerical results here provided cannot be applied to analyze current experiments. However, the physical conclusions reached here are general. Our analysis can be directly extended to study matter systems including several energy levels [60], a collection of quantum emitters, or collective excitations (see, e.g., Ref. [61]) or interacting electron systems [62–64]. Moreover, the conceptual issues discussed and solved here may also apply to light-matter systems involving multimode resonators [54,65–67], or to atoms (natural or artificial) coupled to a continuum of light modes [68], or even in cavity quantum optomechanics [69,70]. Finally, we point out that most of the concepts put forward here can also be applied to circuit QED systems. Some preliminary results can be found in Ref. [71].

ACKNOWLEDGMENTS

A.S., D.Z., and S.H. acknowledge RIKEN for its hospitality, D.Z. acknowledges the support by the Spanish Ministerio de Ciencia, Innovaciòn y Universidades within project MAT2017-88358-C3-1-R, the Aragòn Government project Q-MAD, EU-QUANTERA project SUMO and the Fundaciòn BBVA. F.N. is supported in part by: Nippon Telegraph and Telephone Corporation (NTT) Research, the Japan Science and Technology Agency (JST) [via the Quantum Leap Flagship Program (Q-LEAP) program, the Moonshot R&D Grant No. JPMJMS2061, and the Centers of Research Excellence in Science and Technology (CREST) Grant No. JPMJCR1676], the Japan Society for the Promotion of Science (JSPS) [via the Grants-in-Aid for Scientific Research (KAKENHI) Grant No. JP20H00134 and the JSPS RFBR Grant No. JPJSBP120194828], the Army Research Office (ARO) (Grant No. W911NF-18-1-0358), the Asian Office of Aerospace Research and Development (AOARD) (via Grant No. FA2386-20-1-4069), and the Foundational Questions Institute Fund (FQXi) via Grant No. FQXi-IAF19-06. S.H. acknowledges funding from the Canadian Foundation for Innovation, and the Natural Sciences and Engineering Research Council of Canada. S.S. acknowledges the Army Research Office (ARO) (Grant No. W911NF-19-1-0065).

APPENDIX A: DERIVATION OF THE PHOTON OPERATORS IN THE DIPOLE GAUGE

We start by considering the simplest case of a two-level system (TLS) coupled to a single-mode resonator, where $\hat{a}$ is the photon destruction operator in the Coulomb gauge. Following Ref. [11] (see also Sec. II), the corresponding operator in the dipole gauge is $\hat{a}' = \hat{\mathcal{T}}\hat{a}\hat{\mathcal{T}}^\dagger$, where $\hat{\mathcal{T}} = \exp(i\hat{\mathcal{F}})$ with $\hat{\mathcal{F}} = -\eta\hat{\sigma}_x(\hat{a} + \hat{a}^\dagger)$. We obtain $\hat{a}' = \hat{a} + i\eta\hat{\sigma}_x$, where $\eta = g/\omega_c$ (g is assumed real).

We now check the consistency of this result by deriving the general case using an alternative approach not based on unitary transformations. Specifically, we consider a single TLS interacting with a collection of complete electromagnetic modes, and then generalize the result to a strict single-mode coupling regime.

It is well known [14,36,72] that the dipole interaction Hamiltonian between an atom and the radiation field, should involve the transverse displacement field, $\hat{\mathbf{D}}$, rather than the electric field, $\hat{\mathbf{E}}$, so that (we neglect a μ^2 term that is trivially proportional to the identity operator in a two-level approximation):

$$\hat{\mathcal{H}}_I = -\frac{\boldsymbol{\mu}\cdot\hat{\mathbf{D}}(\mathbf{r})}{\epsilon_0\epsilon_b(\mathbf{r})}, \tag{A1}$$

where $\epsilon_b(\mathbf{r})$ is the background dielectric constant of the medium where the TLS is embedded. The key point is that in the dipole gauge the electric field operator is not a canonical operator and thus the energy has to be expressed in terms of $\hat{\mathbf{D}}(\mathbf{r})$ (which is a canonical operator), in order to obtain the interaction Hamiltonian. Given the displacement field's fundamental importance [37,73], we introduce a new field

operator through

$$\hat{\mathbf{F}}(\mathbf{r}) = \frac{\hat{\mathbf{D}}(\mathbf{r})}{\epsilon_0 \epsilon_b(\mathbf{r})}, \tag{A2}$$

and carry out field quantization with respect to this quantum field operator. Thus, for a single dipole at position $\mathbf{r}_0$,

$$\hat{\mathcal{H}}_I = -\boldsymbol{\mu} \cdot \hat{\mathbf{F}}(\mathbf{r}_0), \tag{A3}$$

and below we assume $\boldsymbol{\mu}$ is real (though this is not necessary). This procedure can be generalized for multiple dipoles; however, in this case the field-induced dipole-dipole interaction terms have to be also included (see Appendix III B). In this section, we only consider a single dipole (TLS) at $\mathbf{r}_0$. The field operator, obtained from the Power-Zienau-Woolley (PZW) transformation, can be expanded in terms of photon field operators (that also couple to matter degrees of freedom), $\hat{a}_k$, so that

$$\begin{aligned}\hat{\mathbf{F}}(\mathbf{r},t) &= \hat{\mathbf{F}}^{+}(\mathbf{r},t) + \hat{\mathbf{F}}^{-}(\mathbf{r},t) \\ &= i\sum_k \sqrt{\frac{\hbar\omega_k}{2\epsilon_0}}\mathbf{f}_k(\mathbf{r})\hat{a}_k(t) + \text{H.c.},\end{aligned} \tag{A4}$$

where $\mathbf{f}_k(\mathbf{r})$ are "normal modes" with real eigenfrequencies, ω_k, obtained from Maxwell's equations for a particular medium. The normalization of these normal modes is obtained from $\int d\mathbf{r}\epsilon_b(\mathbf{r})\mathbf{f}_k^*(\mathbf{r})\cdot\mathbf{f}_{k'}(\mathbf{r}) = \delta_{kk'}$. These modes are complete, so that $\sum_k \epsilon_b(\mathbf{r})\mathbf{f}_k^*(\mathbf{r})\mathbf{f}_k(\mathbf{r}') = \mathbf{1}\delta(\mathbf{r}-\mathbf{r}')$, and note that the sum includes both quasitransverse and quasilongitudinal modes ($\omega_k = 0$). For convenience, one can also write this as

$$\mathbf{1}\delta(\mathbf{r}-\mathbf{r}_0) = \frac{1}{2}\epsilon_b(\mathbf{r})\left[\sum_k \mathbf{f}_k(\mathbf{r})\mathbf{f}_k^*(\mathbf{r}_0) + \mathbf{f}_k^*(\mathbf{r}_0)\mathbf{f}_k(\mathbf{r})\right]. \tag{A5}$$

We can also introduce the usual TLS-mode coupling rate from

$$g_k \equiv \sqrt{\frac{\omega_k}{2\hbar\epsilon_0}}\boldsymbol{\mu}\cdot\mathbf{f}_k(\mathbf{r}_0), \tag{A6}$$

which is only finite for transverse modes (which is due to the choice of gauge).

Next, it is useful to recall the relation between $\hat{\mathbf{E}}$ and $\hat{\mathbf{F}}$:

$$\hat{\mathbf{F}}(\mathbf{r}) = \hat{\mathbf{E}}(\mathbf{r}) + \frac{\delta(\mathbf{r}-\mathbf{r}_0)}{\epsilon_0\epsilon_b(\mathbf{r})}\hat{\mathbf{P}}_d(\mathbf{r}_0), \tag{A7}$$

where we consider a single dipole. Treating the dipole as a quantized TLS, then

$$\hat{\mathbf{F}}(\mathbf{r}) = \hat{\mathbf{E}}(\mathbf{r}) + \frac{\boldsymbol{\mu}}{\epsilon_0\epsilon_b(\mathbf{r})}\delta(\mathbf{r}-\mathbf{r}_0)(\hat{\sigma}_+ + \hat{\sigma}_-), \tag{A8}$$

where $\hat{\sigma}_+ + \hat{\sigma}_- = \hat{\sigma}_x$ are the usual Pauli operators. Thus, defining $\hat{\mathbf{E}}_D(\mathbf{r})$ as the electric field operator in the dipole gauge, we have

$$\begin{aligned}\hat{\mathbf{E}}_D(\mathbf{r},t) &= i\sum_k \sqrt{\frac{\hbar\omega_k}{2\epsilon_0}}\mathbf{f}_k(\mathbf{r})\hat{a}_k(t) + \text{H.c.} \\ &\quad - \frac{1}{2\epsilon_0}\left[\sum_k \mathbf{f}_k(\mathbf{r})\mathbf{f}_k^*(\mathbf{r}_0) + \mathbf{f}_k^*(\mathbf{r}_0)\mathbf{f}_k(\mathbf{r})\right] \\ &\quad \cdot\boldsymbol{\mu}(\hat{\sigma}_+ + \hat{\sigma}_-),\end{aligned} \tag{A9}$$

with the understanding that the last term is formally zero for $\mathbf{r} \neq \mathbf{r}_0$. For positions away from the dipole location, then

$$\hat{\mathbf{E}}_D(\mathbf{r}\neq\mathbf{r}_0,t) = i\sum_k \sqrt{\frac{\hbar\omega_k}{2\epsilon_0}}\mathbf{f}_k(\mathbf{r})\hat{a}_k(t) + \text{H.c.}, \tag{A10}$$

while for positions at the dipole location,

$$\begin{aligned}\hat{\mathbf{E}}_D(\mathbf{r}_0,t) &= i\sum_k \sqrt{\frac{\hbar\omega_k}{2\epsilon_0}}\mathbf{f}_k(\mathbf{r}_0)\hat{a}_k(t) + \text{H.c.} \\ &\quad - \frac{1}{\epsilon_0}\left[\sum_k \mathbf{f}_k^*(\mathbf{r}_0)\mathbf{f}_k(\mathbf{r}_0)\right]\cdot\boldsymbol{\mu}(\hat{\sigma}_+ + \hat{\sigma}_-).\end{aligned} \tag{A11}$$

Also note, that since $\hat{\mathbf{E}}_D(\mathbf{r}\neq\mathbf{r}_0,t) = \hat{\mathbf{F}}(\mathbf{r},t)$, then one can use either operator for field detection analysis (away from the TLS), which is a result of including a sum over all modes. It is also important to note that the general solution of $\hat{a}_k(t)$ also includes coupling to the TLS, which can be obtained, e.g., from the appropriate Heisenberg equations of motion. It is worth noticing that Eq. (A9) can be rewritten in a way that makes each mode contribution more clear:

$$\hat{\mathbf{E}}_D(\mathbf{r},t) = i\sum_k \sqrt{\frac{\hbar\omega_k}{2\epsilon_0}}\mathbf{f}_k(\mathbf{r})\hat{a}'_k(t) + \text{H.c.}, \tag{A12}$$

where

$$\hat{a}'_k(t) = \hat{a}_k(t) + i\eta_k\hat{\sigma}_x, \tag{A13}$$

with $\omega_k\eta_k = \sqrt{\omega_k/2\hbar\epsilon_0}\,\boldsymbol{\mu}\cdot\mathbf{f}_k(\mathbf{r}_0)$. Comparing Eqs. (A12) and (A4), it is clear that, although $\hat{\mathbf{E}}_D(\mathbf{r}\neq\mathbf{r}_0,t) = \hat{\mathbf{F}}(\mathbf{r},t)$, the electric field operator $\hat{\mathbf{E}}_D(\mathbf{r},t)$ and the field $\hat{\mathbf{F}}_D(\mathbf{r},t)$ correspond to two different modal expansions.

1. Single-mode limit

Next, we focus on a single-mode solution ($k = c, \hat{a} \equiv \hat{a}_c, \eta \equiv \eta_c$) as this is typically the most interesting case for cavity QED regimes, and is one of the key models considered in the main text (the quantum Rabi model). Of course, treating a single-field mode as a normal mode is not a rigorous model for open cavities, as we cannot include the cavity mode loss rigorously, but similar result can be obtained using a quantized quasinormal mode approach [74,75] (which are the correct resonant modes in the presence of dissipative output losses). Nevertheless, for high-Q resonators, it is an excellent approximation. Exploiting Eq. (A12), we obtain

$$\hat{\mathbf{E}}_D(\mathbf{r},t) \approx i\sqrt{\frac{\hbar\omega_c}{2\epsilon_0}}\mathbf{f}_c(\mathbf{r})\hat{a}'(t) + \text{H.c.}, \tag{A14}$$

where

$$\hat{a}'(t) = \hat{a}(t) + i\eta\hat{\sigma}_x, \tag{A15}$$

with $\omega_c\eta = \sqrt{\omega_c/2\hbar\epsilon_0}\,\boldsymbol{\mu}\cdot\mathbf{f}_c(\mathbf{r}_0)$. Again assuming that g is real, then $g = \omega_c\eta$, and $\hat{\mathcal{H}}_I = i\hbar g(\hat{a}^\dagger - \hat{a})\hat{\sigma}_x \equiv \hat{\mathcal{V}}_D$, as used in the main text.

It is worth highlighting a rather striking difference between the single-mode model and the multimode model. The latter case causes the two field operators $\hat{\mathbf{F}}_D(\mathbf{r})$ and $\hat{\mathbf{E}}_D(\mathbf{r})$ to be identical, *unless* $\mathbf{r}$ *at the dipole location* ($\mathbf{r}_0$). This multimode

result also enforces some fundamental results in electromagnetism, e.g., it recovers well known limits such as the local field problem (requiring the self-consistent polarization), and ensures causality. The need to enforce causality in quantum optics has been pointed out in other contexts [54]. We also observe that, as shown explicitly by the unitary transformation $\hat{a}' = \hat{T}\hat{a}\hat{T}^\dagger$ at the beginning of this section (see also [11]), by only using the primed operators in the dipole gauge, gauge invariance of the expectation values is ensured. Generalizing this approach to the multimode-interaction case, it can also be shown that $\hat{a}'_k = \hat{T}\hat{a}_k\hat{T}^\dagger$, where $\hat{T}$ is the appropriate unitary gauge operator [17]. Consequently,

$$\langle\psi_D|\hat{a}_k'^\dagger\,\hat{a}'_k|\psi_D\rangle = \langle\psi_C|\hat{a}_k^\dagger\,\hat{a}_k|\psi_C\rangle,$$

where $|\psi_D\rangle = \hat{T}|\psi_C\rangle$.

APPENDIX B: DISPERSIVE READOUT OF A QUBIT STRONGLY COUPLED TO A CAVITY MODE

Let us consider a TLS ultrastrongly coupled to a cavity mode of frequency ω_a and weakly coupled to a second mode (e.g., a readout cavity) of frequency ω_b acting as a sensor for the matter system. As shown in the main text (Sec. IV), the resulting Hamiltonian in the Coulomb gauge can be written as [11]

$$\hat{\mathcal{H}}_C = \hbar\omega_a\hat{a}^\dagger\hat{a} + \hbar\omega_b\hat{b}^\dagger\hat{b} + \frac{\hbar\omega_0}{2}\{\hat{\sigma}_z\cos[2\eta_a(\hat{a}^\dagger+\hat{a}) + 2\eta_b(\hat{b}^\dagger+\hat{b})] + \hat{\sigma}_y\sin[2\eta_a(\hat{a}^\dagger+\hat{a}) + 2\eta_b(\hat{b}^\dagger+\hat{b})]\}, \tag{B1}$$

with $\eta_a = g_a/\omega_0$ and $\eta_b = g_b/\omega_0$. Assuming that $2\eta_b(\hat{b}^\dagger+\hat{b})$ is small as compared to the other terms, as shown in the main text (Sec. IV), we obtain

$$\hat{\mathcal{H}}_C = \hbar\omega_a\hat{a}^\dagger\hat{a} + \hbar\omega_b\hat{b}^\dagger\hat{b} + \frac{\hbar\omega_0}{2}\hat{\sigma}_z^C + \eta_b\hbar\omega_0(\hat{b}^\dagger+\hat{b})\hat{\sigma}_y^C, \tag{B2}$$

where the Pauli operators in the Coulomb gauge $\hat{\sigma}_i^C$ have been defined in Eq. (26). Moreover, we define

$$\hat{\mathcal{X}}_\pm^C = (\hat{b}^\dagger\hat{\sigma}_-^C \pm \hat{b}\hat{\sigma}_+^C),$$
$$\hat{\mathcal{Y}}_\pm^C = (\hat{b}\hat{\sigma}_-^C \pm \hat{b}^\dagger\hat{\sigma}_+^C). \tag{B3}$$

Subsequently, Eq. (B2) can be rewritten in a more convenient form as

$$\hat{\mathcal{H}}_C = \hbar\omega_a\hat{a}^\dagger\hat{a} + \hbar\omega_b\hat{b}^\dagger\hat{b} + \frac{\hbar\omega_0}{2}\hat{\sigma}_z^C + i\eta_b\hbar\omega_0(\hat{\mathcal{X}}_-^C + \hat{\mathcal{Y}}_-^C). \tag{B4}$$

In order to investigate the effect of the readout cavity on the TLS, we can always perform a canonical (unitary) transformation (see, e.g., Ref. [53]):

$$\hat{\mathcal{H}}_C \to \tilde{\mathcal{H}}_C \equiv e^{-\hat{S}}\hat{\mathcal{H}}_C e^{\hat{S}} = \hat{\mathcal{H}}_C + [\hat{\mathcal{H}}_C,\hat{S}] + \frac{1}{2!}[\hat{S},[\hat{S},\hat{\mathcal{H}}_C]] + \ldots, \tag{B5}$$

where we defined $\tilde{\mathcal{H}}_C$ to indicate the corresponding dispersive Hamiltonian in the Coulomb gauge. In the usual way, we search for an anti-Hermitian operator $\hat{S}$ which satisfies the relation

$$\hat{\mathcal{H}}_I + [\hat{\mathcal{H}}_0,\hat{S}] = 0, \tag{B6}$$

where

$$\hat{\mathcal{H}}_I = i\eta_b\hbar\omega_0(\hat{\mathcal{X}}_-^C + \hat{\mathcal{Y}}_-^C) \tag{B7}$$

and

$$\hat{\mathcal{H}}_0 = \hbar\omega_b\hat{b}^\dagger\hat{b} + \frac{\hbar\omega_0}{2}\hat{\sigma}_z^C. \tag{B8}$$

Equation (B6) is satisfied using

$$\hat{S} = \lambda\hat{\mathcal{X}}_+^C + \bar{\lambda}\hat{\mathcal{Y}}_+^C, \tag{B9}$$

with

$$\lambda = -i\frac{g_b}{\Delta} \tag{B10}$$

and

$$\bar{\lambda} = -i\frac{g_b}{\Sigma}, \tag{B11}$$

where $\Delta = \omega_0 - \omega_b$ and $\Sigma = \omega_0 + \omega_b$. With such a choice, we obtain

$$\tilde{\mathcal{H}}_C = \hbar\omega_a\hat{a}^\dagger\hat{a} + \hat{\mathcal{H}}_0 + [\hat{\mathcal{H}}_I,\hat{S}] + \frac{1}{2!}[\hat{S},[\hat{S},\hat{\mathcal{H}}_C]] + \ldots \tag{B12}$$

Developing the calculations up to the second order in g_b, we obtain

$$\tilde{\mathcal{H}}_C = \hat{\mathcal{H}}_0^C + \frac{\hbar\chi}{2}(\hat{b}^\dagger+\hat{b})^2\,\hat{\sigma}_z^C, \tag{B13}$$

where

$$\chi = \frac{g_b^2}{\Delta} + \frac{g_b^2}{\Sigma} \tag{B14}$$

and

$$\hat{\mathcal{H}}_0^C = \hbar\omega_a\hat{a}^\dagger\hat{a} + \hbar\omega_b\hat{b}^\dagger\hat{b} + \frac{\hbar\omega_0}{2}\hat{\sigma}_z^C. \tag{B15}$$

Neglecting the counter-rotating terms proportional to $\hat{b}^{\dagger 2}$ and $\hat{b}^2$, Eq. (B13) becomes

$$\tilde{\mathcal{H}}_C = \hbar\omega_a\hat{a}^\dagger\hat{a} + \left(\frac{\hbar\omega_0}{2} - \frac{\hbar\chi}{2}\right)\hat{\sigma}_z^C + \hbar\big(\omega_b + \chi\hat{\sigma}_z^C\big)\hat{b}^\dagger\hat{b}. \tag{B16}$$

As it is clear from this expression, the last term in Eq. (B16) can be interpreted as a dispersive shift of the cavity transition by $\chi\hat{\sigma}_z^C$, depending on the state of the qubit [76]. Sending a frequency-tunable probe signal into the resonator b, transmission spectroscopy can provide direct information on the expectation value $\langle\hat{\sigma}_z^C\rangle_C$ which coincides with $\langle\hat{\sigma}_z\rangle_D$. Hence, we can conclude that this kind of readout spectroscopy provides direct information on the expectation value of the qubit population difference, as defined in the dipole gauge.

APPENDIX C: LARGE-COUPLING LIMIT

Here we discuss the large-coupling limit ($\eta \gg 1$) by using an analytical perturbative method. Notice that for $\eta \gg 1$, the system enters in the so-called deep strong coupling (DSC) regime. We start from the quantum Rabi Hamiltonian in the dipole gauge:

$$\hat{\mathcal{H}}_D = \hat{\mathcal{H}}_{\rm free} + \hat{\mathcal{V}}_D, \tag{C1}$$

where

$$\hat{\mathcal{H}}_{\rm free} = \hbar\omega_c\hat{a}^\dagger\hat{a} + \frac{\hbar\omega_0}{2}\hat{\sigma}_z, \tag{C2}$$

and the interaction Hamiltonian is

$$\hat{\mathcal{V}}_D = i\eta\hbar\omega_c(\hat{a}^\dagger - \hat{a})\hat{\sigma}_x. \tag{C3}$$

When $\eta\omega_c \gg \omega_0$, the last term in Eq. (C1) can be regarded as a perturbation. Equation (C2) can be rewritten as $\hat{\mathcal{H}}_D = \hat{\mathcal{H}}_0' + \hat{\mathcal{V}}_D'$, where

$$\hat{\mathcal{H}}_0' = \hbar\omega_c\hat{a}^\dagger\hat{a} + i\eta\hbar\omega_c(\hat{a}^\dagger - \hat{a})\hat{\sigma}_x \tag{C4}$$

and

$$\hat{\mathcal{V}}_D' = \frac{\hbar\omega_0}{2}\hat{\sigma}_z. \tag{C5}$$

In the limit $\eta \gg 1$, $\hat{\mathcal{V}}_D'$ can be regarded as a small perturbation; neglecting it, the resulting Hamiltonian can be analytically diagonalized. The two resulting lowest-energy degenerate eigenstates can be written as $|\mp i\eta\rangle|\pm_x\rangle$, where the first ket indicates photonic coherent states with amplitude $\mp i\eta$, such that: $\hat{a}|\mp i\eta\rangle = \mp i\eta|\mp i\eta\rangle$; while the second ket indicates the eigenstates of $\hat{\sigma}_x$. The perturbation $(\hbar\omega_0/2)\hat{\sigma}_z$ removes the degeneracy and mixes the two states, so that the two eigenstates become entangled:

$$|\psi_D^\pm\rangle = \frac{1}{\sqrt{2}}[|-i\eta\rangle|+_x\rangle \pm |+i\eta\rangle|-_x\rangle]. \tag{C6}$$

The corresponding eigenstates in the Coulomb gauge are $|\psi_C^\pm\rangle = \hat{\mathcal{T}}^\dagger|\psi_D^\pm\rangle$, where

$$\hat{\mathcal{T}} = \exp[-i\eta(\hat{a} + \hat{a}^\dagger)\hat{\sigma}_x] \tag{C7}$$

is the unitary operator determining the gauge transformation of the qubit-oscillator system: $\mathcal{H}_D = \hat{\mathcal{T}}H_C\hat{\mathcal{T}}^\dagger$. By applying the operator $\hat{\mathcal{T}}^\dagger$ to both members of Eq. (C6), and using the properties of the displacement operator, we obtain the separable states

$$|\psi_C^\pm\rangle = |0\rangle|\pm_z\rangle. \tag{C8}$$

Equations (C6) and (C8), describing the lowest two energy states in the dipole and Coulomb gauge respectively (for $\eta \gg 1$), explain the results in Figs. 4 and 5 for very large values of η. In particular, it is easy to obtain: $\langle\psi_C^-|\hat{\sigma}_+\hat{\sigma}_-|\psi_C^-\rangle = 0$, $\langle\psi_C^+|\hat{\sigma}_+\hat{\sigma}_-|\psi_C^+\rangle = 1$, $\langle\psi_D^\pm|\hat{\sigma}_+\hat{\sigma}_-|\psi_D^\pm\rangle = 0.5$, $\langle\psi_C^-|\hat{a}^\dagger\hat{a}|\psi_C^-\rangle = 0$, $\langle\psi_C^+|\hat{a}^\dagger\hat{a}|\psi_C^+\rangle = \eta^2$. Moreover, Eq. (C6) describes two light-matter maximally entangled cat states providing a qubit entropy $S_D^q = 1$, while Eq. (C8) describes two separable states ($S_C^q = 0$), see Fig. 5.

APPENDIX D: GAUGE TRANSFORMATIONS IN THE PRESENCE OF TIME-DEPENDENT COUPLING

We start by summarizing some well-known results on equivalent descriptions of the dynamics of a physical system (see, e.g., Ref. [17]). We consider a simple 1D dynamical system described by the Lagrangian $L(x, \dot{x})$, where x is the coordinate and $\dot{x}$ the velocity. The momentum conjugate with x is $p = \partial L/\partial x$. By adding to the Lagrangiaan $L(x, \dot{x})$ the total time derivative of a function $F(x, t)$, one obtains a new Lagrangian

$$L'(x, \dot{x}) = L(x, \dot{x}) + \frac{d}{dt}F(x, t) = L(x, \dot{x}) + \dot{x}\frac{\partial F}{\partial x} + \frac{\partial F}{\partial t}, \tag{D1}$$

which is equivalent to L in the sense that it gives the same equation of motion for the coordinate x. Considering the new Lagrangian, the momentum conjugate with x becomes

$$p' = \frac{\partial L'}{\partial \dot{x}} = p + \frac{\partial F}{\partial x}. \tag{D2}$$

When one applies the standard canonical quantization procedure, starting with L on the one hand and L' on the other, one derives two equivalent quantum descriptions for the system, related by a unitary transformation, described by the operator (we use $\hbar = 1$)

$$\hat{T} = \exp[i\hat{F}(t)], \tag{D3}$$

where $\hat{F}(t) \equiv F(\hat{x}, t)$ is the quantum operator corresponding to the classical function $F(x, t)$, with the hat "ˆ" indicating the promotion of classical variables to quantum operators. Considering a generic operator $\hat{O} = O(\hat{x}, \hat{p})$, it transforms as $\hat{O}' = \hat{T}\hat{O}\hat{T}^\dagger$, while the state vectors transform as $|\psi'\rangle = \hat{T}|\psi\rangle$, so that the generic matrix elements of the operators remain unchanged. If the function $F(x, t)$ depends explicitly on time, the system Hamiltonain transforms differently:

$$\hat{H}' = \hat{T}\hat{H}\hat{T}^\dagger + i\dot{\hat{T}}\hat{T}^\dagger = \hat{T}\hat{H}\hat{T}^\dagger - \frac{\partial\hat{F}}{\partial t}. \tag{D4}$$

The function F introduced by PZW [35,72] is

$$F = -\int d^3r\, \mathbf{P}(\mathbf{r}) \cdot \mathbf{A}_\perp(\mathbf{r}), \tag{D5}$$

where, considering a single charge centered on a single reference point $\mathbf{R}$, the polarization operator can be expressed as

$$\mathbf{P}(\mathbf{r}) = q\int_0^1 du(\mathbf{r} - \mathbf{R})\delta[(1 - u)(\mathbf{r} - \mathbf{R})]. \tag{D6}$$

Hence, the PZW Lagrangian can be derived by that in the Coulomb gauge by the transformation

$$L' = L + \frac{d}{dt}F, \tag{D7}$$

where F is given by Eq. (D5).

In a gauge transformation, defined by a function $\chi(\mathbf{r}, t)$, the potentials become

$$\mathbf{A}'(\mathbf{r}, t) = \mathbf{A}(\mathbf{r}, t) + \nabla\chi(\mathbf{r}, t), \tag{D8a}$$

$$U'(\mathbf{r}, t) = U(\mathbf{r}, t) - \frac{\partial}{\partial t}\chi(\mathbf{r}, t). \tag{D8b}$$

Introducing Eqs. (D8a) and (D8b) in the Lagrangian L in the Coulomb gauge, the following relationship between the two Lagrangians holds (see, e.g., p. 267 of Ref. [17]):

$$L' = L + \frac{d}{dt}\chi(\mathbf{r}, t). \tag{D9}$$

If the function $\chi(\mathbf{r}, t)$ is chosen equal to the function $F(\mathbf{r}, t)$, then

$$\chi(\mathbf{r}, t) = -\int d^3r\, \mathbf{P}(\mathbf{r}) \cdot \mathbf{A}_\perp(\mathbf{r}). \tag{D10}$$

Equations (D7) and (D9) shows that the PZW transformation and the multipolar gauge transformation are equivalent. This equivalence still holds in the presence of a time-dependent interaction strength. As discussed in the main text, an example of a time-dependent coupling can be properly

described assuming an atom moving in and out a Fabry-Pérot Gaussian cavity mode, like in experiments with Rydberg atoms [77], so that the coupling strength becomes time dependent. In this case, the charge is localized around a time-dependent position $\mathbf{R}(t)$. This will give rise to additional terms when taking the time derivative of F. However, Eqs. (D7) and (D9) do still coincide, as do the conjugate momenta. Both approaches give rise to the same Hamiltonian in Eq. (D4). Notice that the resulting Hamiltonian after the gauge transformation is different from

$$\hat{H}_D(t) = \hat{T}(t)\hat{H}_C(t)\hat{T}^\dagger(t). \tag{D11}$$

This explains precisely why the Hamiltonian in Eq. (D11) does not describe dynamics which is equivalent to that of the Hamiltonian in the Coulomb gauge [32]. In short, Eq. (D11) is not the correct Hamiltonian to describe the correct light-matter interaction dynamics. Specifically, considering the time-dependent unitary transformation, Eq. (D11) is incorrect because it misses the explicit time dependence on the transformation—see last term in Eq. (D4). The gauge transformation, Eq. (D11) is not correct because it is obtained by neglecting the explicit time dependence of $\chi(\mathbf{r}, t)$ in Eq. (D8b), arising from the time dependence of $\mathbf{R}$ in Eq. (D6). The correct Hamiltonian in the dipole gauge, in the presence of time-dependent interactions, is

$$\hat{H}'_D = \hat{T}(t)\hat{H}_C(t)\hat{T}^\dagger(t) + i\dot{\hat{T}}\hat{T}^\dagger.$$

Further analysis and some examples of the consequences can be found in Sec. V.

APPENDIX E: NONADIABATIC TUNABLE COUPLING: SWITCH-ON AND SWITCH-OFF DYNAMICS

Following Ref. [32], we consider the treatment of tuneable light-matter interactions through a time-dependent coupling function. In Ref. [32], it is shown that applying the standard procedure, for sufficiently strong light-matter interactions, the final subsystem properties, such as entanglement and subsystem energies, depend significantly on the definitions (gauges) of light and matter adopted during their interaction. This occurs even if the interaction is not present at the initial and final stages of the protocol, at which times the subsystems are uniquely defined and can be individually addressed. Such an ambiguity is surprising and poses serious doubts on the predictability of the system dynamics in the presence of ultrastrong time-dependent light-matter interactions.

Here we address this apparent problem by considering a light-atom system initially in the absence of interaction and starting, e.g., in its ground state $|\psi(t_{\rm in})\rangle = |g, 0\rangle$. A different choice of the initial state does not change the conclusions. This situation can be visualized considering a system consistenting of an optical cavity (initially prepared in the zero-photon state) and an atom initially external to the cavity and in its ground state. At $t = t_1$, the atom enters the cavity and leaves it at $t = t_2$. We consider the case of a TLS (the generalization to multilevel systems is straightforward). In addition, for the sake of simplicity, we assume that for $t_1 < t < t_2$, the normalized interaction strength η is constant. We will demonstrate that: *after one switches off the interaction, the same quantum state is obtained independently of the adopted gauge.*

We start our analysis considering the Coulomb gauge. The initial state (actually independent on the gauge) is $|\psi_C(t_{\rm in})\rangle = |g, 0\rangle_C$. At $t = t_1$, the interaction is nonadiabatically switched on within a time $T \to 0$. This sudden switch has no effect on the quantum state [55], hence, at $t = t_1^+ = t_1 + T$, $|\psi_C(t_1^+)\rangle = |g, 0\rangle$. For $t > t_1^+$, the quantum state evolves as $|\psi_C(t)\rangle = \exp[-i\hat{\mathcal{H}}_C(t - t_1)]|g, 0\rangle_C$. Then, at $t = t_2$, the interaction is suddenly switched off. At $t = t_2^+ = t_2 + T$, the system state is $|\psi_C(t_2^+)\rangle = \exp[-i\hat{\mathcal{H}}_C(t_2 - t_1)]|g, 0\rangle_C$. For $t > t_2$, the quantum state evolves according to the Hamiltonian for the noninteracting system ($\eta = 0$): $|\psi_C(t)\rangle = \exp[-i\hat{\mathcal{H}}_{\rm free}(t - t_2)]|\psi_C(t_2^+)\rangle$, where $\mathcal{H}_{\rm free}$ is the system Hamiltonian in the absence of interaction. We can use these quantum states to calculate any system expectation value at any time. For example, the mean photon number can be calculated as

$$\langle\psi_C(t)|\hat{Y}^{(-)}\hat{Y}^{(+)}|\psi_C(t)\rangle, \tag{E1}$$

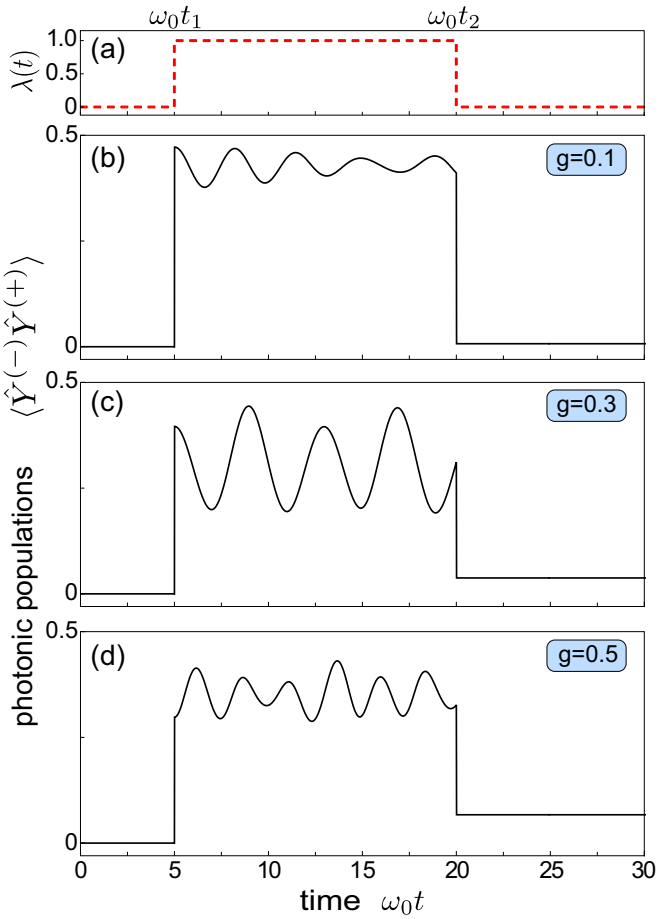

FIG. 6. Gauge-invariant emission of a TLS coupled to a single-mode resonator (quantum Rabi Hamiltonian) induced by sudden switching on and off the light-matter interaction, calculated for three normalized coupling strengths. (a) Displays the switching function $\lambda(t)$. The system is initially prepared in its ground state: $|\psi_C(t_{\rm in})\rangle = |g, 0\rangle$. At $t = t_1$, the interaction is suddenly switched on, and it is finally switched off at $t = t_2$. (b)–(d) display $\langle\psi_C(t)|\hat{Y}^{(-)}\hat{Y}^{(+)}|\psi_C(t)\rangle$ for three different coupling strengths.

where $\hat{Y}^{(+)}$ and $\hat{Y}^{(-)}$ are the positive and negative-frequency components of the operator $\hat{Y} = i(\hat{a} - \hat{a}^\dagger)$ [with $\hat{Y}^{(-)} = (\hat{Y}^{(+)})^\dagger$]. Notice that, for $t < t_1$ and $t > t_2$, $\hat{Y}^{(+)} = i\hat{a}$.

Now we describe the same dynamics in the dipole gauge. Before switching on the interaction, the state is simply $|\psi_D(t_1^-)\rangle = |g, 0\rangle$. As shown in Appendix D, the system Hamiltonian in the dipole gauge is

$$\begin{aligned}\hat{\mathcal{H}}_D(t) &= \hat{\mathcal{T}}(t)\hat{\mathcal{H}}_C\hat{\mathcal{T}}^\dagger(t) + i\dot{\hat{\mathcal{T}}}(t)\hat{\mathcal{T}}^\dagger(t) \\ &= \hat{\mathcal{H}}_{\text{free}} + \hat{\mathcal{V}}_D(t) - \dot{\lambda}\hat{\mathcal{F}}, \end{aligned} \tag{E2}$$

where $\lambda(t)$ is the switching function (see Fig. 6). Notice that, when the interaction strength is time independent, the last term in Eq. (E2) goes to zero. However, during nonadiabatic switches or modulations, this term can become the dominant one. Owing to the presence of the last term in Eq. (E2), the state after the switch-on of the interaction becomes

$$|\psi_D(t_1^+)\rangle = \exp\left(i\hat{\mathcal{F}}\int_{t_1^-}^{t_1^+} dt\,\dot{\lambda}\right)|\psi_D(t_1^-)\rangle = \hat{\mathcal{T}}|g, 0\rangle. \tag{E3}$$

For $t > t_1^+$, the quantum state evolves as $|\psi_D(t)\rangle = \exp(-i\hat{\mathcal{H}}_D(t - t_1)\hat{\mathcal{T}}|g, 0\rangle$. Then, at $t = t_2$, the interaction is suddenly switched off. At $t = t_2^+ = t_2 + T$ the system state becomes $|\psi_D(t_2^+)\rangle = \hat{\mathcal{T}}^\dagger \exp[-i\hat{\mathcal{H}}_D(t_2 - t_1)]\hat{\mathcal{T}}|g, 0\rangle$. Since $\hat{\mathcal{H}}_C = \hat{\mathcal{T}}^\dagger\hat{\mathcal{H}}_D\hat{\mathcal{T}}$, it implies that

$$|\psi_D(t_2^+)\rangle = |\psi_C(t_2^+)\rangle. \tag{E4}$$

As an example, we show in Fig. 6 the gauge-invariant emission,

$$\langle\psi_C(t)|\hat{Y}^{(-)}\hat{Y}^{(+)}|\psi_C(t)\rangle,$$

from a TLS coupled to a single-mode resonator (quantum Rabi Hamiltonian) induced by sudden switching on and off the light-matter interaction, calculated for three normalized coupling strengths.

As a final remark, we observe that the procedure described here can be directly extended to show that gauge invariance is also preserved for intermediate gauge transformations dependent on a continuous parameter α [10]. Indeed, it is sufficient to replace $\hat{\mathcal{F}}$ with $\alpha\hat{\mathcal{F}}$.

[1] A. F. Kockum, A. Miranowicz, S. D. Liberato, S. Savasta, and F. Nori, Ultrastrong coupling between light and matter, Nat. Rev. Phys. **1**, 19 (2019).

[2] P. Forn-Díaz, L. Lamata, E. Rico, J. Kono, and E. Solano, Ultrastrong coupling regimes of light-matter interaction, Rev. Mod. Phys. **91**, 025005 (2019).

[3] A. Bayer, M. Pozimski, S. Schambeck, D. Schuh, R. Huber, D. Bougeard, and C. Lange, Terahertz light-matter interaction beyond unity coupling strength, Nano Lett. **17**, 6340 (2017).

[4] F. Yoshihara, T. Fuse, S. Ashhab, K. Kakuyanagi, S. Saito, and K. Semba, Superconducting qubit-oscillator circuit beyond the ultrastrong-coupling regime, Nat. Phys. **13**, 44 (2017).

[5] R. Chikkaraddy, B. de Nijs, F. Benz, S. J. Barrow, O. A. Scherman, E. Rosta, A. Demetriadou, P. Fox, O. Hess, and J. J. Baumberg, Single-molecule strong coupling at room temperature in plasmonic nanocavities, Nature (London) **535**, 127 (2016).

[6] A. Bisht, J. Cuadra, M. Wersäll, A. Canales, T. J. Antosiewicz, and T. Shegai, Collective strong light-matter coupling in hierarchical microcavity-plasmon-exciton systems, Nano Lett. **19**, 189 (2018).

[7] P.-H. Ho, D. B. Farmer, G. S. Tulevski, S.-J. Han, D. M. Bishop, L. M. Gignac, J. Bucchignano, P. Avouris, and A. L. Falk, Intrinsically ultrastrong plasmon–exciton interactions in crystallized films of carbon nanotubes, Proc. Natl. Acad. Sci. USA **115**, 12662 (2018).

[8] D. Ballester, G. Romero, J. J. García-Ripoll, F. Deppe, and E. Solano, Quantum Simulation of the Ultrastrong-Coupling Dynamics in Circuit Quantum Electrodynamics, Phys. Rev. X **2**, 021007 (2012).

[9] D. De Bernardis, P. Pilar, T. Jaako, S. De Liberato, and P. Rabl, Breakdown of gauge invariance in ultrastrong-coupling cavity QED, Phys. Rev. A **98**, 053819 (2018).

[10] A. Stokes and A. Nazir, Gauge ambiguities imply Jaynes-Cummings physics remains valid in ultrastrong coupling QED, Nat. Commun. **10**, 499 (2019).

[11] O. Di Stefano, A. Settineri, V. Macrì, L. Garziano, R. Stassi, S. Savasta, and F. Nori, Resolution of gauge ambiguities in ultrastrong-coupling cavity QED, Nat. Phys. **15**, 803 (2019).

[12] L. Garziano, A. Settineri, O. Di Stefano, S. Savasta, and F. Nori, Gauge invariance of the Dicke and Hopfield models, Phys. Rev. A **102**, 023718 (2020).

[13] W. E. Lamb, Fine structure of the hydrogen atom. III, Phys. Rev. **85**, 259 (1952).

[14] W. P. Healy, Comment onelectric dipole interaction in quantum optics, Phys. Rev. A **22**, 2891 (1980).

[15] E. A. Power and T. Thirunamachandran, Comment on electric dipole interaction in quantum optics, Phys. Rev. A **22**, 2894 (1980).

[16] W. E. Lamb, R. R. Schlicher, and M. O. Scully, Matter-field interaction in atomic physics and quantum optics, Phys. Rev. A **36**, 2763 (1987).

[17] C. Cohen-Tannoudji, J. Dupont-Roc, and G. Grynberg, *Photons and Atoms: Introduction to Quantum Electrodynamics* (Wiley-VCH, New York, 1997).

[18] S. Savasta, O. Di Stefano, A. Settineri, D. Zueco, S. Hughes, and F. Nori, Gauge principle and gauge invariance in quantum two-level systems, arXiv:2006.06583 [Phys. Rev. A (to be published)] (2021).

[19] R. J. Glauber, The quantum theory of optical coherence, Phys. Rev. **130**, 2529 (1963).

[20] J. Keeling, Coulomb interactions, gauge invariance, and phase transitions of the Dicke model, J. Phys.: Condens. Matter **19**, 295213 (2007).

[21] A. Vukics and P. Domokos, Adequacy of the Dicke model in cavity QED: A counter-no-go statement, Phys. Rev. A **86**, 053807 (2012).

[22] S. Ashhab and F. Nori, Qubit-oscillator systems in the ultrastrong-coupling regime and their potential for preparing nonclassical states, Phys. Rev. A **81**, 042311 (2010).

[23] R. Stassi, A. Ridolfo, O. Di Stefano, M. J. Hartmann, and S. Savasta, Spontaneous Conversion from Virtual to Real Photons in the Ultrastrong-Coupling Regime, Phys. Rev. Lett. **110**, 243601 (2013).

[24] S. De Liberato, Virtual photons in the ground state of a dissipative system, Nat. Commun. **8**, 1465 (2017).

[25] O. Di Stefano, R. Stassi, L. Garziano, A. F. Kockum, S. Savasta, and F. Nori, Feynman-diagrams approach to the quantum Rabi model for ultrastrong cavity QED: Stimulated emission and reabsorption of virtual particles dressing a physical excitation, New J. Phys. **19**, 053010 (2017).

[26] C. Ciuti, G. Bastard, and I. Carusotto, Quantum vacuum properties of the intersubband cavity polariton field, Phys. Rev. B **72**, 115303 (2005).

[27] S. De Liberato, C. Ciuti, and I. Carusotto, Quantum Vacuum Radiation Spectra from a Semiconductor Microcavity with a Time-Modulated Vacuum Rabi Frequency, Phys. Rev. Lett. **98**, 103602 (2007).

[28] L. Garziano, A. Ridolfo, R. Stassi, O. Di Stefano, and S. Savasta, Switching on and off of ultrastrong light-matter interaction: Photon statistics of quantum vacuum radiation, Phys. Rev. A **88**, 063829 (2013).

[29] L. Garziano, R. Stassi, V. Macrì, A. F. Kockum, S. Savasta, and F. Nori, Multiphoton quantum Rabi oscillations in ultrastrong cavity QED, Phys. Rev. A **92**, 063830 (2015).

[30] G. Falci, A. Ridolfo, P. G. Di Stefano, and E. Paladino, Ultrastrong coupling probed by coherent population transfer, Sci. Rep. **9**, 9249 (2019).

[31] E. Sánchez-Burillo, L. Martín-Moreno, J. J. García-Ripoll, and D. Zueco, Single Photons by Quenching the Vacuum, Phys. Rev. Lett. **123**, 013601 (2019).

[32] A. Stokes and A. Nazir, Ultrastrong time-dependent light-matter interactions are gauge relative, Phys. Rev. Research **3**, 013116 (2021).

[33] K. G. Wilson, Confinement of quarks, Phys. Rev. D **10**, 2445 (1974).

[34] U.-J. Wiese, Ultracold quantum gases and lattice systems: Quantum simulation of lattice gauge theories, Ann. Phys. **525**, 777 (2013).

[35] M. Babiker and R. Loudon, Derivation of the Power-Zienau-Woolley Hamiltonian in quantum electrodynamics by gauge transformation, Proc. R. Soc. London A **385**, 439 (1983).

[36] J. M. Wylie and J. E. Sipe, Quantum electrodynamics near an interface, Phys. Rev. A **30**, 1185 (1984).

[37] M. Wubs, L. G. Suttorp, and A. Lagendijk, Multiple-scattering approach to interatomic interactions and superradiance in inhomogeneous dielectrics, Phys. Rev. A **70**, 053823 (2004).

[38] O. Di Stefano, A. F. Kockum, A. Ridolfo, S. Savasta, and F. Nori, Photodetection probability in quantum systems with arbitrarily strong light-matter interaction, Sci. Rep. **8**, 17825 (2018).

[39] A. Ridolfo, M. Leib, S. Savasta, and M. J. Hartmann, Photon Blockade in the Ultrastrong Coupling Regime, Phys. Rev. Lett. **109**, 193602 (2012).

[40] L. Garziano, A. Ridolfo, S. De Liberato, and S. Savasta, Cavity QED in the ultrastrong coupling regime: Photon bunching from the emission of individual dressed qubits, ACS Photonics **4**, 2345 (2017).

[41] S. Savasta, O. D. Stefano, and F. Nori, Thomas–Reiche–Kuhn (TRK) sum rule for interacting photons, Nanophotonics **10**, 465 (2020).

[42] W. Salmon, C. Gustin, A. Settineri, O. D. Stefano, D. Zueco, S. Savasta, F. Nori, and S. Hughes, Gauge-independent emission spectra and quantum correlations in the ultrastrong coupling regime of cavity-QED, arXiv:2102.12055.

[43] E. del Valle, A. Gonzalez-Tudela, F. P. Laussy, C. Tejedor, and M. J. Hartmann, Theory of Frequency-Filtered and Time-Resolved *n*-Photon Correlations, Phys. Rev. Lett. **109**, 183601 (2012).

[44] C. Schäfer, M. Ruggenthaler, V. Rokaj, and A. Rubio, Relevance of the quadratic diamagnetic and self-polarization terms in cavity quantum electrodynamics, ACS Photonics **7**, 975 (2020).

[45] M. Brune, S. Haroche, V. Lefevre, J. M. Raimond, and N. Zagury, Quantum Nondemolition Measurement of Small Photon Numbers by Rydberg-Atom Phase-Sensitive Detection, Phys. Rev. Lett. **65**, 976 (1990).

[46] M. Brune, S. Haroche, J. M. Raimond, L. Davidovich, and N. Zagury, Manipulation of photons in a cavity by dispersive atom-field coupling: Quantum-nondemolition measurements and generation of "Schrödinger cat" states, Phys. Rev. A **45**, 5193 (1992).

[47] P. Grangier, J. A. Levenson, and J.-P. Poizat, Quantum non-demolition measurements in optics, Nature (London) **396**, 537 (1998).

[48] M. Boissonneault, J. M. Gambetta, and A. Blais, Dispersive regime of circuit QED: Photon-dependent qubit dephasing and relaxation rates, Phys. Rev. A **79**, 013819 (2009).

[49] F. Helmer, M. Mariantoni, E. Solano, and F. Marquardt, Quantum nondemolition photon detection in circuit QED and the quantum Zeno effect, Phys. Rev. A **79**, 052115 (2009).

[50] B. Peaudecerf, T. Rybarczyk, S. Gerlich, S. Gleyzes, J. M. Raimond, S. Haroche, I. Dotsenko, and M. Brune, Adaptive Quantum Nondemolition Measurement of a Photon Number, Phys. Rev. Lett. **112**, 080401 (2014).

[51] A. Blais, R.-S. Huang, A. Wallraff, S. M. Girvin, and R. J. Schoelkopf, Cavity quantum electrodynamics for superconducting electrical circuits: An architecture for quantum computation, Phys. Rev. A **69**, 062320 (2004).

[52] S. Haroche and J.-M. Raimond, *Exploring the Quantum* (Oxford University Press, 2006).

[53] D. Zueco, G. M. Reuther, S. Kohler, and P. Hänggi, Qubit-oscillator dynamics in the dispersive regime: Analytical theory beyond the rotating-wave approximation, Phys. Rev. A **80**, 033846 (2009).

[54] C. S. Muñoz, F. Nori, and S. De Liberato, Resolution of superluminal signalling in non-perturbative cavity quantum electrodynamics, Nat. Commun. **9**, 1924 (2018).

[55] A. Messiah, *Quantum Mechanics* (Dover Publications, 1999).

[56] F. Assemat, D. Grosso, A. Signoles, A. Facon, I. Dotsenko, S. Haroche, J. M. Raimond, M. Brune, and S. Gleyzes, Quantum Rabi Oscillations in Coherent and in Mesoscopic Cat Field States, Phys. Rev. Lett. **123**, 143605 (2019).

[57] M. Maggiore, *A Modern Introduction to Quantum Field Theory*, Oxford Series in Physics No. 12 (Oxford University Press, 2005).

[58] R. Stassi and F. Nori, Long-lasting quantum memories: Extending the coherence time of superconducting artificial atoms in the ultrastrong-coupling regime, Phys. Rev. A **97**, 033823 (2018).

[59] R. Stassi, M. Cirio, and F. Nori, Scalable quantum computer with superconducting circuits in the ultrastrong coupling regime, npj Quantum Inf. **6**, 67 (2020).

[60] M. A. D. Taylor, A. Mandal, W. Zhou, and P. Huo, Resolution of Gauge Ambiguities in Molecular Cavity Quantum Electrodynamics, Phys. Rev. Lett. **125**, 123602 (2020).

[61] D. De Bernardis, T. Jaako, and P. Rabl, Cavity quantum electrodynamics in the nonperturbative regime, Phys. Rev. A **97**, 043820 (2018).

[62] G. M. Andolina, F. M. D. Pellegrino, V. Giovannetti, A. H. MacDonald, and M. Polini, Cavity quantum electrodynamics of strongly correlated electron systems: A no-go theorem for photon condensation, Phys. Rev. B **100**, 121109(R) (2019).

[63] G. M. Andolina, F. M. D. Pellegrino, V. Giovannetti, A. H. MacDonald, and M. Polini, Theory of photon condensation in a spatially varying electromagnetic field, Phys. Rev. B **102**, 125137 (2020).

[64] O. Dmytruk and M. Schiró, Gauge fixing for strongly correlated electrons coupled to quantum light, Phys. Rev. B **103**, 075131 (2021).

[65] N. M. Sundaresan, Y. Liu, D. Sadri, L. J. Szőcs, D. L. Underwood, M. Malekakhlagh, H. E. Türeci, and A. A. Houck, Beyond Strong Coupling in a Multimode Cavity, Phys. Rev. X **5**, 021035 (2015).

[66] M. Malekakhlagh, A. Petrescu, and H. E. Türeci, Cutoff-Free Circuit Quantum Electrodynamics, Phys. Rev. Lett. **119**, 073601 (2017).

[67] A. F. Kockum, V. Macrì, L. Garziano, S. Savasta, and F. Nori, Frequency conversion in ultrastrong cavity QED, Sci. Rep. **7**, 5313 (2017).

[68] P. Forn-Díaz, J. J. García-Ripoll, B. Peropadre, J.-L. Orgiazzi, M. A. Yurtalan, R. Belyansky, C. M. Wilson, and A. Lupascu, Ultrastrong coupling of a single artificial atom to an electromagnetic continuum in the nonperturbative regime, Nat. Phys. **13**, 39 (2017).

[69] C. K. Law, Interaction between a moving mirror and radiation pressure: A Hamiltonian formulation, Phys. Rev. A **51**, 2537 (1995).

[70] V. Macrì, A. Ridolfo, O. Di Stefano, A. F. Kockum, F. Nori, and S. Savasta, Nonperturbative Dynamical Casimir Effect in Optomechanical Systems: Vacuum Casimir-Rabi Splittings, Phys. Rev. X **8**, 011031 (2018).

[71] A. Settineri, O. Di Stefano, D. Zueco, S. Hughes, S. Savasta, and F. Nori, Gauge freedom, quantum measurements, and time-dependent interactions in cavity and circuit QED, arXiv:1912.08548.

[72] E. A. Power and T. Thirunamachandran, Quantum electrodynamics in a cavity, Phys. Rev. A **25**, 2473 (1982).

[73] P. Yao, C. Van Vlack, A. Reza, M. Patterson, M. M. Dignam, and S. Hughes, Ultrahigh Purcell factors and Lamb shifts in slow-light metamaterial waveguides, Phys. Rev. B **80**, 195106 (2009).

[74] S. Franke, S. Hughes, M. K. Dezfouli, P. T. Kristensen, K. Busch, A. Knorr, and M. Richter, Quantization of Quasinormal Modes for Open Cavities and Plasmonic Cavity Quantum Electrodynamics, Phys. Rev. Lett. **122**, 213901 (2019).

[75] S. Franke, M. Richter, J. Ren, A. Knorr, and S. Hughes, Quantized quasinormal-mode description of nonlinear cavity-QED effects from coupled resonators with a Fano-like resonance, Phys. Rev. Research **2**, 033456 (2020).

[76] R. Bianchetti, S. Filipp, M. Baur, J. M. Fink, M. Göppl, P. J. Leek, L. Steffen, A. Blais, and A. Wallraff, Dynamics of dispersive single-qubit readout in circuit quantum electrodynamics, Phys. Rev. A **80**, 043840 (2009).

[77] S. Haroche, Nobel lecture: Controlling photons in a box and exploring the quantum to classical boundary, Rev. Mod. Phys. **85**, 1083 (2013).